AIAA 2025 - 2026 Aircraft Design Proposal

Next-Generation Carrier-based Strike Fighter Aircraft

Student Chapter of AIAA at UT Austin

YFQ - 75 Trident

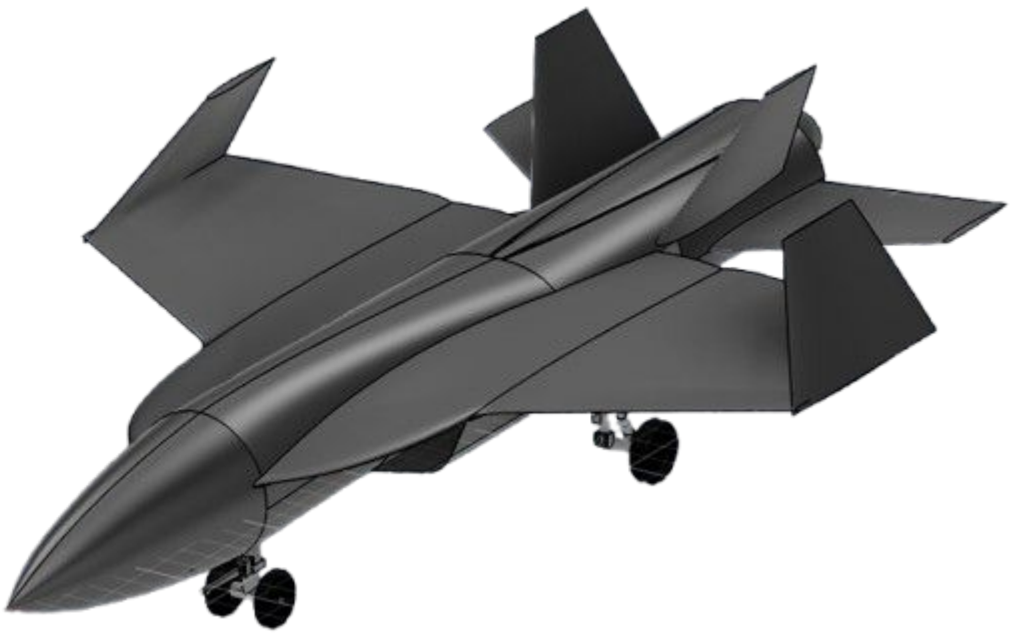

TEXAS
The University of Texas at Austin
AIAA

I. Table of Contents

II. Team Overview

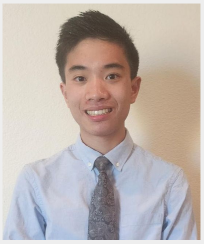
William S.

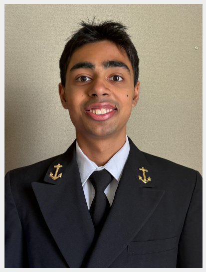
Arjun R.


Sujay S.


Ramaakshay M.


Abhi C.


Sneha S.


Jacob J.


Amaan D.


Shrey J.


Greg Z.

Team Member	Position	Sub-Team	AIAA	Signature
William S.	Chief Engineer	Overview	1745172	William Su
Arjun R.	Team Lead	Vehicle	1922579	Arjun Rajesh
Sujay S.	System Integration	Vehicle	1921851	Sujay Sahoo
Ramaakshay M.	Propulsion	Vehicle	1921866	Ramaakshay Mallireddy
Abhi C.	Team Lead	Mission	1921857	Abhijith C
Sneha S.	Cost Analysis	Mission	1899150	Sneha Shrestha
Jacob J.	Maintenance	Mission	1921850	Jacob Jimenez
Amaan D.	Mass Analysis	Mission	1922008	Amaan Desai
Shrey Joshi	Undergraduate Mentor	-	-	Shrey Joshi
Greg Zwernemann	Professor of Practice, Faculty Advisor	-	19751	Greg Zwernemann

III. Introduction

Since its introduction with the Navy in 1999, the aging F/A-18E/F Super Hornet is in dire need of a modern replacement to meet the modern threats and combat missions required for a carrier-based strike aircraft in the 21st century. The YFQ-75 Trident emerged from this glaring vulnerability with the intent of improving the air-to-air and strike capabilities of naval strike aircraft, while also developing emerging technologies such as unmanned aerial systems, and being more cost affordable and production-oriented than its vaunted predecessors. In the following report, the Aircraft Design Competition Bureau of the UT Austin Chapter of the American Institute of Aeronautics and Astronautics will record, among other things, the design philosophy, capabilities, metrics, and simulated performance of the YFQ-75 Trident.

IV. Design Philosophy

The Request for Proposal set forth by the Navy places a strong emphasis on Augustine's Law which highlights the increasing acquisition cost of strike fighter aircraft over time (AIAA Aircraft Design Technical Committee 1). There is also a heavy emphasis on matching and improving the mission profiles and characteristics of the now aging F/A 18-E/F Super Hornet. Such metrics include compatibility with the current CVN-68 and CVN-78 carriers in addition to a maximum speed of mach 1.6 at 30,000 feet with a considerable payload outfit of 4 MK-83 JDAMs and 2 AIM-9Cs (AIAA Aircraft Design Technical Committee 2-4). In light of these developments, this design bureau aims to design a naval strike aircraft which can meet, and even exceed the objectives required through the use of radical technologies such as a composite frame and unmanned control system while keeping the procurement cost of this vehicle equivalent to that of a U.S. fighter aircraft such as the F-35A in the year 2000 which sets a benchmark value of $100,000,000. This objective can be summed up into designing, a naval strike aircraft with higher costs than the contemporary F/A-18E/F Super Hornet but with increased capabilities to match the objectives put forth by the Request for Proposal. More crucially, while the procurements costs may be considerably higher than the Super Hornet it will be below the modern procurement costs of aircraft, while also boosting the performance of the vehicle through the aforementioned design features which keeps the aircraft, as small, versatile, and efficient as possible.

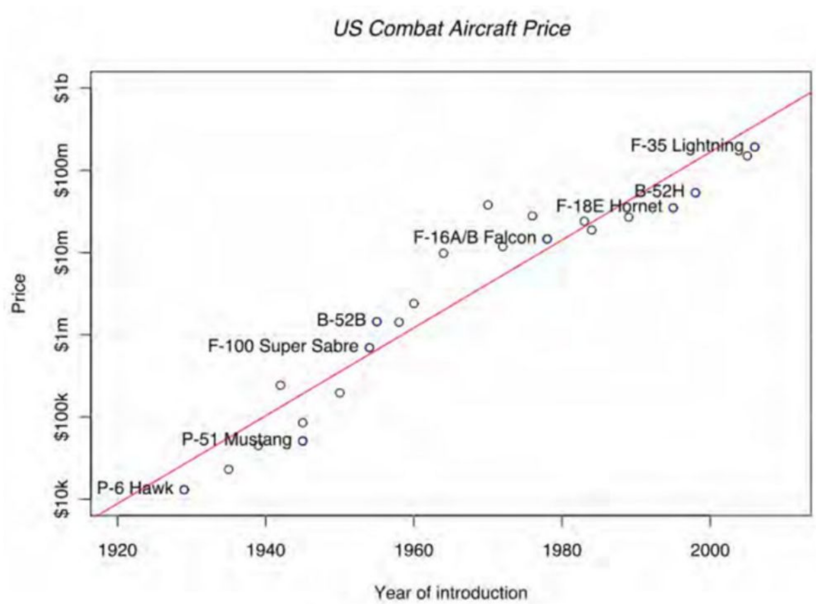

Figure 1: AIAA Aircraft Design Technical Committee "US Combat Aircraft Price"

V. Core Tenets

A. Preface

Going into this design project, the key has firmly remained in balancing the cost and capability of the aircraft. To achieve this end, the capability of the YFQ-75 can be broken down into three main aspects: survivability, detectability, and lethality. In the following sections this design bureau will demonstrate how each was balanced to ensure that the YFQ-75 is optimized to be as capable and cost-effective as possible.

B. Detectability

Detectability is primarily concerned with evading the search of radars, infrared tracking sensors, or optical search system. Traditionally, this is solved through the a combination of systems such as radar-absorbing paint, geometrical shaping, and engine baffles which minimize the radar cross section and the infrared signature of the plane. For this report, radar-absorbing paint and other stealth systems will not be incorporated due to the lack of public information on these technologies, but geometrical shaping and engine baffles will be incorporated into the design to reduce detectability as much as possible. Additionally, a powerful electronics warfare suite will be incorporated into the airframe to reduce the range at which the YFQ-75 can be detected when conducting missions. The following systems and their characteristics will be elaborated on in the geometric configuration section of this report.

C. Survivability

When it comes to the YFQ-75, survivability can be summarized as the ability of our airplane to avoid incoming threats once detected by radars, infrared tracking sensors, or optical search systems. This manifests itself in the maximum speed and maneuverability of the vehicle. As specified by the RFP, the desired max speed of the airframe is at least Mach 1.6 at 30,000 feet with a minimum sustained turn rate of 8 degrees per second at 20,000 feet (AIAA Aircraft Design Technical Committee 4). For the YFQ-75 we aimed to meet and exceed these metrics to boost the survivability of our aircraft with a powerful engine and a durable composite frame to sustain higher turn rates at higher gravitational forces. The survivability characteristics of the aircraft will be elaborated on in the airframe and engine section of this report.

D. Lethality

For the YFQ-75, lethality comes in the form of versatility. As an unmanned aerial system, it can be outfitted with a wide variety of engagement options to conduct a broad scope of missions which would be too dangerous for conventional aircraft. As per the Request for Proposal, the base YFQ-75 will come with 4 Mk-83 JDAMs and 2 AIM-9Cs for the strike profile while 6 AIM-120Ds and 2 AIM-9Cs will be implemented for the air-to-air profile (AIAA Aircraft Design Technical Committee 3-4). To supplement the lethality of the strike profile a targeting pod and advanced optical tracking systems will be incorporated into the aircraft while the beyond visual range capabilities of the YFQ-75 will be bolstered through the use of an AESA radar for the air-to-air profile. The lethality of the aircraft will be elaborated on in the weapons profile section of this report.

VI. Practical Implementation

A. Overview

In this section this design bureau will detail how the aforementioned tenets and design philosophy manifest themselves into the design to match the objectives of the Request for Proposal. In many ways this section will justify the more radical design decisions for the YF-75 such as its unmanned nature, composite frame, and overall layout.

B. Unmanned Aerial Vehicles

Unmanned aerial vehicles from crude commercial drones to MQ-1 Predators have seen an increasing presence on the battlefield. Both abroad and at home, vehicles such as Russia's S-70 Okhotnik-B to Anduril's YFQ-44A demonstrate that the future lies in unmanned systems. This design bureau aims to implement an autonomous control system both to save cost and ensure that the YFQ-75 remains viable throughout the 21st century. Studies have noted that compared to their manned contemporaries, unmanned systems with similar capabilities are far more cost-affordable (Allen 1). This technology then promises to help us stay below the procurement cost threshold of $100,000,000 while maintaining our lethality.

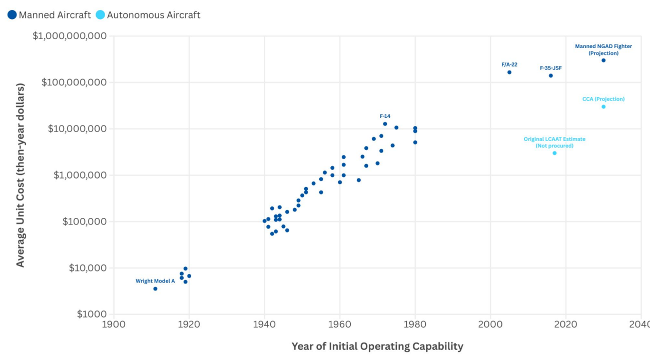

Figure 1: CSIS "Updating Augustine's Law: Fighter Aircraft Cost Growth in the Age of AI and Autonomy"

C. Composite Airframes

Similar to the point made for an autonomous control system, composite airframes have begun to see incremental implementation in vehicles such as the F-35 (Northrop Grumman 1). The YFQ-75 aims to employ a fully composite airframe to reduce the weight of the aircraft which would boost fuel efficiency, payload capacity, and operational range. This is demonstrated when employed on the F-35, composites were noted to having exceptional fatigue strength, resistance to abrasion, and good electrical properties all while being lighter than their contemporaries (Afzal 1).

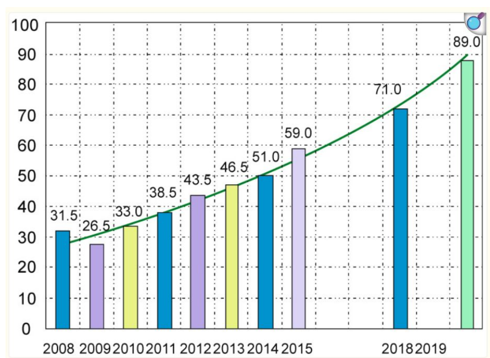

Figure 2: "Practical Use of Composite Materials Used in Military Aircraft

D. Design Layout

The design layout will be expanded on in the following section. That being said, the aircraft was designed to exceed the performance metric and objectives of the Request for Proposal while keeping costs beneath the procurement costs for a fighter aircraft in the benchmark year 2000. This resulted in the aircraft having a low drag coefficient and being as small and lightweight as possible. It has been established previously that aircraft which are lighter and more efficient have lower operating costs and better overall performance (Yeung 1).

VII. Preliminary Vehicle Design

A. Design Overview

As previously mentioned all aircraft design choices were focused on a specific philosophy aimed to field a low cost, highly capable fighter jet to reach RFP requirements. The main driving factors of our design was the high target combat radius of 1,000 nm, the desired dash speed of Mach 1.8, and low speed performance to ensure carrier operability.

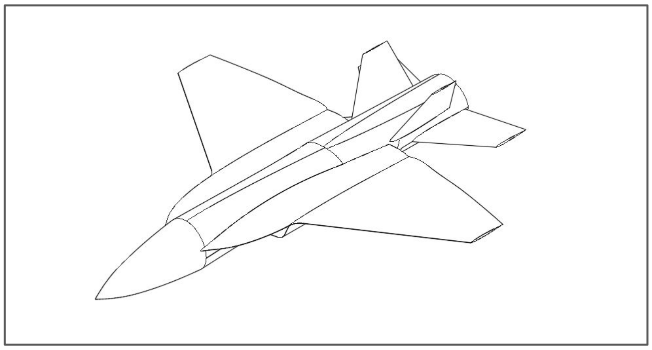

Figure 7. Isometric View YFQ-75

B. Wing Configuration

The preliminary wing geometry chosen for the YFQ-75 blends a trapezoidal shape into the signature delta to achieve an even mix of low speed stability and high speed performance. Leading edge root extensions were added to extend from the root of the wing to the quarter span to induce greater lift at high AoA. A 29° leading edge sweep back was implemented from the quarter span to the root as a mix between the F-15s delta leading edge sweep back and the conservative 22° leading edge sweep back in the F/A-18. The wing was optimized this way to allow for a preliminary blend between the stability and high alpha landings for carrier operability provided by the F-18s wings and the high speed performance offered by the F-15s.

	Stall Speed (0.3)	Cruise Efficiency (0.1)	Low Speed Maneuverability (0.3)	Sustained Turn Rate (0.1)	Deck Footprint (0.15)	Supersonic Drag (0.05)	Weight Scores
80 lb/ft^2	5	2	4	5	1	2	3.65
88 lb/ft^2	4	4	4	4	3	4	3.85
97 lb/ft^2	2	5	1	2	4	3	2.35

Figure 3. Wing Loading Trade Study

A trade study was done to determine the optimal wing loading and was the driving dimension in determining wing span, aspect ratio, and reference area. The selected wing loading of 88 psf excelled in certain preferred fields such low speed stability and stall speed, while mixing good performance in supersonic drag and reduced deck footprint.

Using the predetermined wing loading optimized for the RFP requirements and a target design gross weight of 45,000 lbs, through standard preliminary equations, a initial wing span and wing area were calculated. The chosen aspect ratio to represent our wing was estimated based off of Raymer's Ch.4 for fighter jets.

Intial Variable	Value
Wing Area (S_{ref})	380 ft^2
Wing Span (b)	35.88 ft
Aspect Ratio (AR)	3.4

Figure 8. Initial Sizing Values

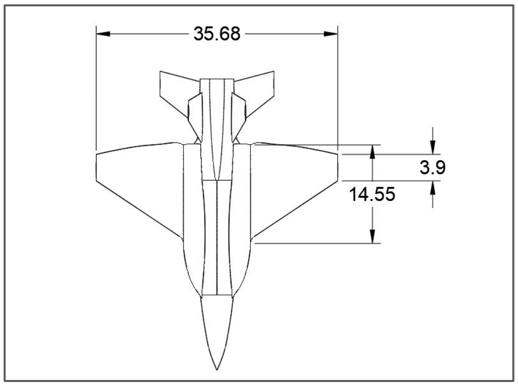

Figure 9. Wing Dimensioning Sketches

C. Fuselage Design

Since YFQ-75 does not have a pilot or internal weapons storage, the aircraft features a streamlined fuselage designed around fitting primarily the radar, landing gear, electronics, avionics, and fuel tanks. According to Raymer's, the recommended fineness ratio for supersonic aircraft ranges from 10-12. The YFQ-75 was designed with a target fineness ratio of 10, featuring a total length of 43ft and a maximum fuselage diameter of approximately 4.4 ft to ensure proper internal storage for all required components.

The YFQ-75 also follows the Supersonic Area Rule to decrease wave drag at mach speeds, featuring a tapered fuselage at the wing roots.

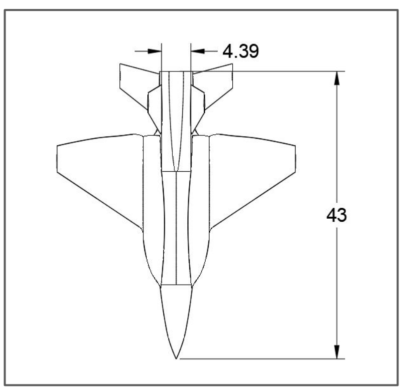

Figure 10. Fuselage Dimensioning Sketch

D. Tail Sizing

The horizontal and vertical tails were both sized as stabilizers for the fighter jet using multiple standard procedures and equations to ensure a preliminary conceptual proof of concept. \

The horizontal stabilizer was sized using the Raymer's Volume Coefficient method. Using Raymer's chart on Horizontal Tail Volume Coefficients, a base Volume coefficient was selected modeled after the F/A -18 at 0.49.

No	Aircraft	Type	Mass (kg)	Wing area (m^2)	Overall length (m)	$\overline{V}_H$
1	Cessna 172	Light GA (Piston)	1,100	16.2	7.9	0.76
2	Piper PA-46-350P	Light transport (Piston)	1,950	16.26	8.72	0.66
3	Alenia G222	Turboprop transport	28,000	82	22.7	0.85
4	Fokker 100	Jet transport	44,000	93.5	35.5	1.07
5	Lake LA-250	Amphibian	1,424	15.24	9.04	0.8
6	Boeing 747-400	Jet transport	362,000	541	73.6	0.81
7	Airbus 340-200	Jet transport	257,000	363.1	59.39	1.11
8	Pilatus PC-12	Turboprop transport	4,100	25.81	14.4	1.08
9	Eurofighter 2000	Fighter	21,000	50	15.96	0.063
10	F/A-18	Fighter	29,937	46.45	18.31	0.49

Figure 11. Raymer's Horizontal Tail Volume Coefficient Chart

To find the planform area of the horizontal tail, the Volume Coefficient Formula was used as referenced in Raymer's Tail. sizing procedure.

$$S_{h,v} = (V_{h,v} * c * S_{ref}) / L_{h,v}$$

Where L_h represents the moment arm from the aerodynamic chord of the wing to the aerodynamic chord of the horizontal stabilizer. Selecting a ratio for l/L, the value of the moment arm over the length of the overall aircraft, of 0.35, standard for a engine inside of the fuselage configuration, a initial L_h can be found to be 19.35ft which would place our total horizontal tail planform area at 74.32 ft^2.

The shaping of the horizontal stabilizer was based simply off the stabilator of the F/A-18 to provide similar pitching moment and aerodynamic properties. This shape features a trapezoidal wing with a 5° steeper leading edge sweep back than the main wing of the YFQ-75.

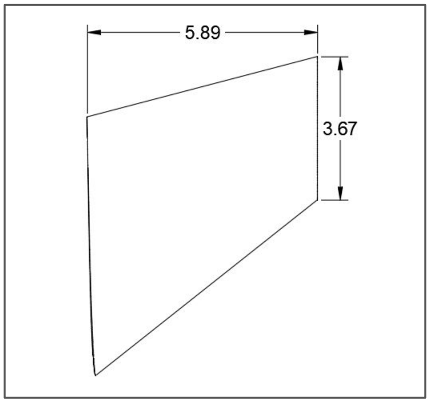

Figure 12. Horizontal Tail Dimensioning Sketch

Sizing for the Vertical Tail was determined in a similar procedure, Raymer's Volume Tail Coefficient. Using a similarly found standard vertical tail volume coefficient for fighter jets around 0.7 and Tail Volume Coefficient equation previously mentioned, the preliminary planform area of the vertical tail was calculated to be 32.2ft^2.

Mentioned in Raymer's Ch.6, fighter jets tend to feature a 20° outward cant of their vertical stabilizers. To calculate the exact area which will be canted we can use the equation mentioned below.

$$S_{panel} = S_v / \cos^2(\theta)$$

We can find the required panel area of the vertical tail to be 41.7ft^2, to account for the 20° outward tilt on the stabilizers.

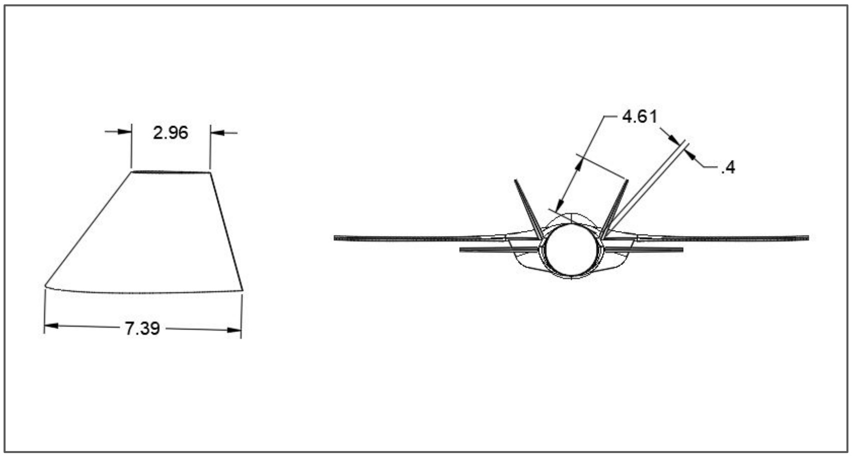

Figure 13. Vertical Stabilizer Dimensioning Sketches

VIII. Control Surface Sizing

A. Elevator

As used most commonly in fighter jet, the prescribed elevator will be an all moving stabilator which will act as the horizontal stabilizer and elevator for the aircraft. To allow for tight high-G turns, and proper maneuverability, the entire stabilizer will act as the main pitching force.

B. Rudder

To initially size the aircraft, the following equation was used and a constant k_r was chosen to be 0.3, a standard rudder coefficient to allow for fighter jet maneuverability as stated in Raymer's Ch.6. Using the chosen Rudder coefficient and the planform reference area of the vertical tail, a preliminary rudder area was calculated.

$$S_r = k_r * S_h$$

After the preliminary rudder area of 15.2 ft^2 was calculated using the chosen rudder coefficient, yaw authority of the aircraft was solved for to determine if rudder power was adequate.

$$\text{Restoring Moment} = S_{ref} * q * C_{n\delta r} * \delta_r * b$$

Where the $C_{n\delta r}$ represented the Rudder control power derivative in terms of time. Using the Helmbold Equation and, and assuming an efficiency of 0.55 and the span factor of 0.9 for the rudder, we can calculate 2d lift curve slope and an estimation of the Rudder Control Power Derivative. With the Aspect Ratio of the vertical tail equaling 0.878 and assuming an initial mach correlation factor of 1.0, $C_{n\delta r}$= 0.00077 rad/s.

With the estimated roll power derivative, the restoring moment of the rudder was calculated to be 24975 lbf, more than enough to properly turn and maneuver our aircraft as required for fighter jets.

C. Aileron

The aileron sizing in a similar matter, required the calculation of the roll power derivative using a simplified equation provided by Raymer's.

$$C_{l\delta a}\text{: Roll Power derivative} = (2 * C_{la,w} * \tau * S_{ail} * y_{ail})/(S*b)$$

The variable $C_{la,w}$ represented the lift curve slope which was estimated using the chosen airfoil Lift vs alpha slope. Through the roll power derivative the steady roll rate estimate was solved for at an aileron deflection of 22°, in combat envelope, speed around mach 0.8. Using the calculated Roll power derivative, $C_{l\delta a}$ = -0.0807, and a steady roll rate of 180° /sec in combat envelope, a requirement provided by Raymer's for fighter jets, we calculated the area of the aileron to be 16.36 ft^2.

$$\text{P: Stead roll rate} = ((C_{l\delta a} * \delta_a)/C_{lp}) * 2V/b$$

The aileron area was tested at carrier approach speeds, and proved to provide a steady roll rate of 61°/sec, which represents proof of concept of the aileron sizing providing the YFQ-75 with more than enough maneuverability to make slight corrections on short final.

D. Flaps

To ensure carrier catapult takeoff capabilities and high alpha approach, the flaps were sized and iterated to prove carrier operability of the YFQ-75. Assuming the landing weight with full ordinance of 30,000 lbs, we can find the required C_L for approach conditions.

$$C_L = LW/(q*S_{ref})$$

The approach C_L required for the YFQ-75 is 2.1. The NACA65005 airfoil at α = 7°, provides a C_L of 0.76. The lift required from the flaps must reach the total C_L for the YFQ-75 to follow through with its carrier approach, meaning the flaps must provide a ΔC_L of 1.34.

Assuming Raymer's equation 12.21 to calculate the lift generated by the flaps as follows, and assuming a flap area of 32 ft^2 initially, the $C_{LFlaps} = 0.42$.

$$\Delta C_L = \Delta c_L * (S_{flaps}/S_{ref}) * \cos(\theta)$$

Since more lift is required for the YFQ-75's approach, the chosen area for the flaps is iterated to 73 ft^2, which provides a total ΔC_L of 0.89, still falling short of the required ΔC_L of 0.45 for the flaps. Due to this, slats were also chosen to be implemented into the wing as another control surface. The surface area of the slats adds is 68ft^2 bringing the total ΔC_L of all control surfaces to 1.4, which provides our aircraft with enough lift to land.

IX. Aerodynamic Parameters

After all initial sizing and design was complete, the YFQ-75 configuration and control surface sizing was simulated in OpenVSP software, VSPAero, to provide proof of stability, maneuverability, and essential aerodynamic variables.

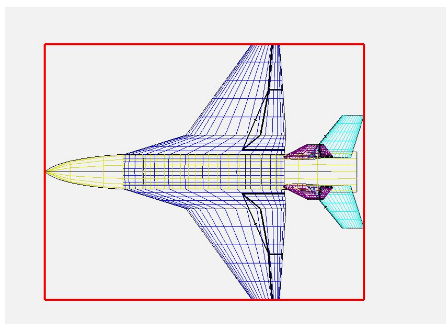

A. Pitching Analysis

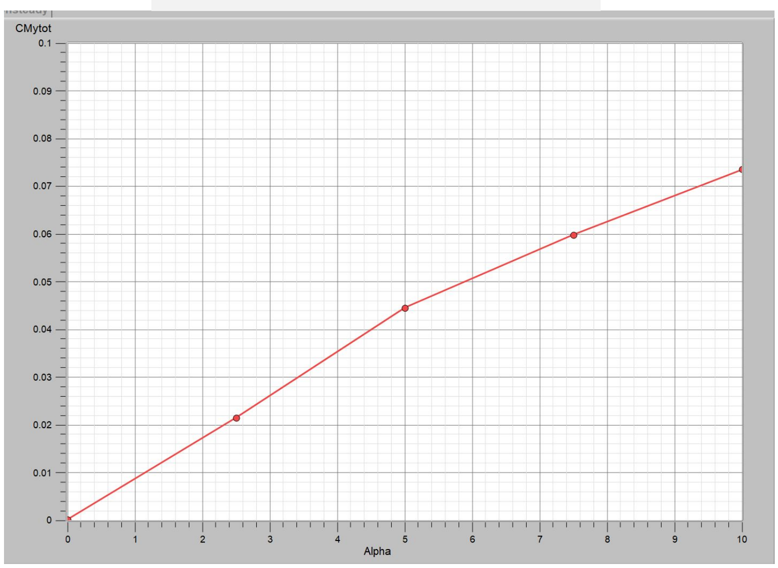

Figure 14. Pitching Moment Vs. Alpha Curve

The graph curve proves slight instability in the YQF-75 as proven by the following positive slope. The Cm_{α} equals 0.0053 per degree, a value acceptable for fighter jets maintained in stability by a fly-by-wire system. Since the YFQ-75 is operating autonomously, it will already have a fly-by wire system implemented to make the slight micro adjustments to keep the aircraft stable.

B. Rolling Analysis

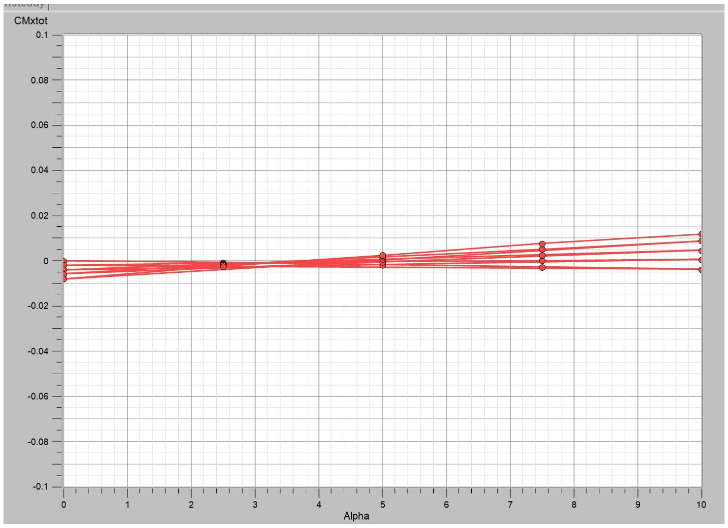

Figure 15. Rolling moment vs Alpha, Static ailerons

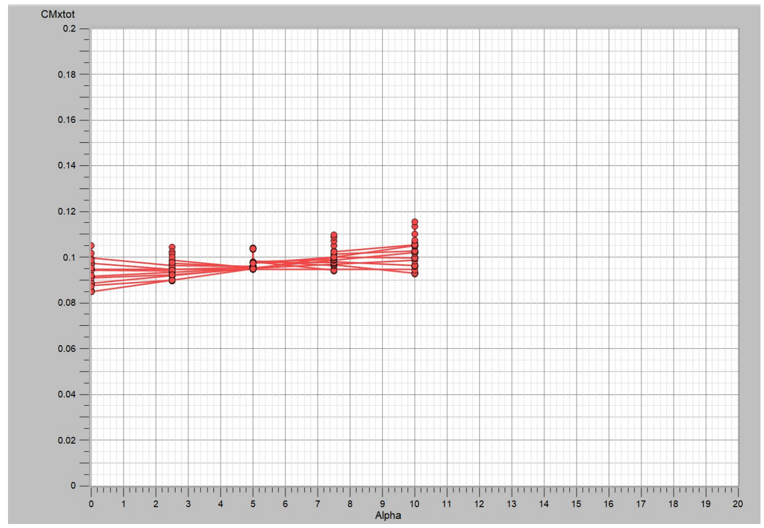

Figure 16. Rolling moment vs. Alpha, Deflected ailerons

After running Beta tests with n=0 to 10, two values were found, Initial Cmx ≈ 0, while the deflected final Cmx ≈ 0.085. To calculate the exact roll power derivative we can divide the change the rolling moment by the change in aileron deflection to find the roll power derivative equals 0.2435 per degree. This value is slightly larger than the estimated value previously calculated via Raymer's equation meaning the ailerons provide more roll than previously established.

Furthermore, after running P analysis, the YFQ-75 was found to have a roll dampening of -0.32, which helps us calculate the true steady roll rate at combat speed to be 646°/sec, which proves high level of roll authority for the aircraft.

C. Yaw Analysis

To determine the directional stability of the aircraft, the moment in the z-axis, Cmz, was plotted against beta, slideslipe, at a cruise alpha of 3°. As shown in Figure 18 by the negative slope, the aircraft is directionally stable and resists yawing.

To find yaw authority, analysis was run with rudders at 0° deflection and 25° of deflection, by dividing the difference in moment by the deflection, the yaw power derivative can be calculated to be -0.0036 per radian, slightly higher than the calculated estimate. Furthermore as shown in Figure 17, the graph crosses the x-axis at a beta of 2.5, meaning that this is our trim angle, and the rudder provides enough corrective moment to counteract slideslipe.

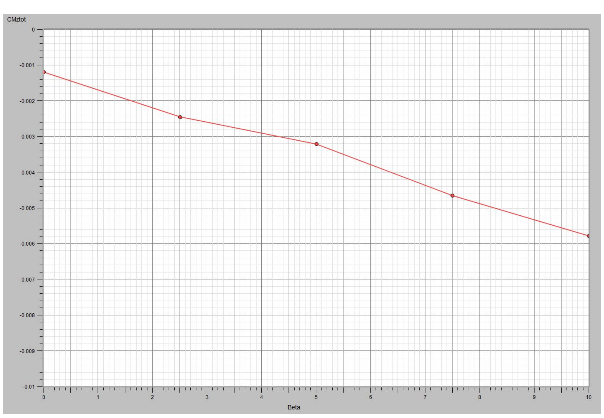

Figure 17. Yaw Power Derivative

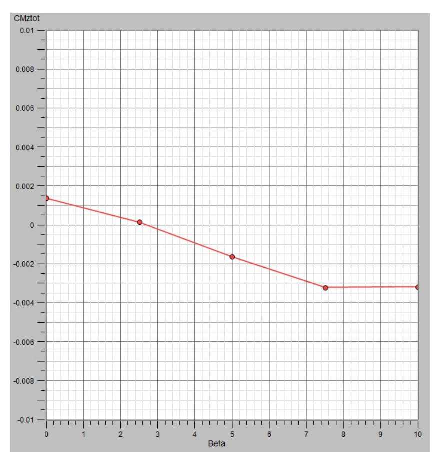

Figure 18. Yaw stability graph

D. Drag Analysis

As found from the Vortex lattice method, the induced drag on the aircraft is 0.02487, and the parasitic drag is 0.0007. This means that the total Cd acting on the plane is 0.032. Shown in the drag polar graph, the zero-lift induced drag is 0.0007 and the max C_L is 0.65.

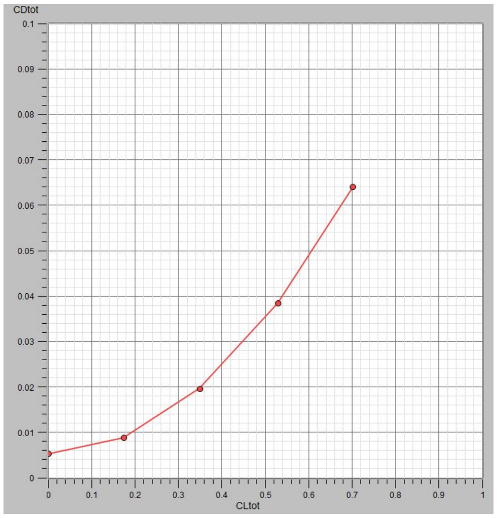

Figure 19. Drag Polar Graph

E. Lift Analysis

The YFQ-75 demonstrates a linear lift curve slope at alpha values from 0-10. Using the graph we can find our lift curve slope to be 4.01 per radian. Since a VLM analysis was done, and predicts no lift separation, exact C_L max cannot be found without higher fidelity simulation.

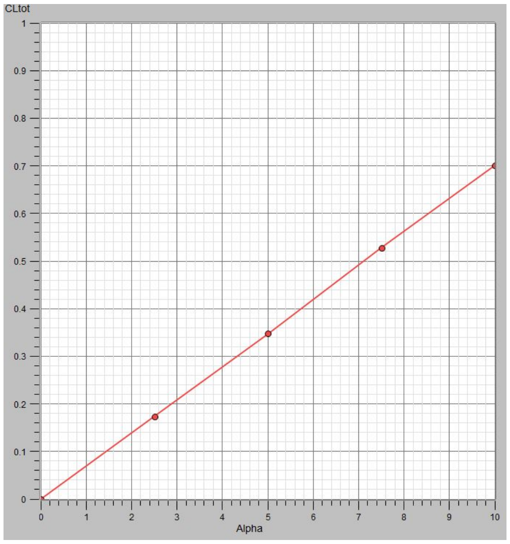

Figure 20. CL Vs. Alpha Curve

X. Internal Configuration

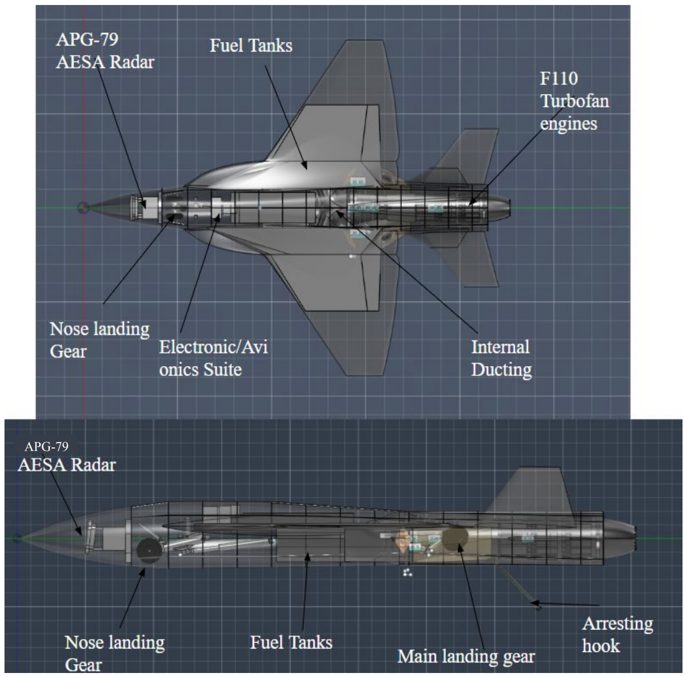

Figure 21. Internal Layout

The YFQ-75 holds, its main AESA radar, internal fuel tanks, electronics and avionics suite, an F110 Turbofan engine, and all three landing gears internally. All internals were laid out and configured with the center of gravity and capacity in mind.

A. Ducting

The ducting which carries the airflow from the trapezoidal intakes to the F110 Turbofan engine was modeled off the F/A-18 and standard fighter jet S-ducts to reduce detectability and help maintain consistent airflow for the engines. The trapezoidal intakes and also based off of the F/A-18.

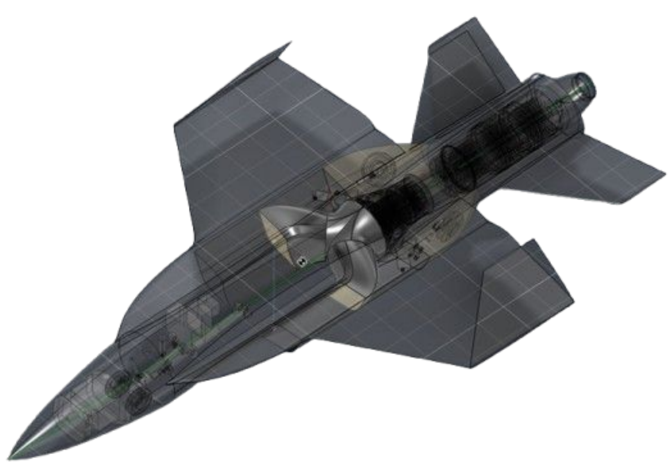

Figure 22. Internal Engine Ducting

B. Airframe

The YFQ-75's airframe is made up of patterns of ribs and spars going across the length of the fuselage and the through the wing. High stress ribs were identified such as at the root wing and engine case holding and thickened to handle higher load cases.

Each standard rib is dimensioned to 0.01 ft of thickness while high stress ribs area thickened to 0.03 ft. The material chosen for the airframe and skin of the aircraft is a carbon composite selected due to its high strength to weight ratio. Although generating a higher cost for the jet, the composite material allows the aircraft to be much lighter compared to standard aircraft grade material such as Aluminum 7075.

Figure 23. Wing Frame

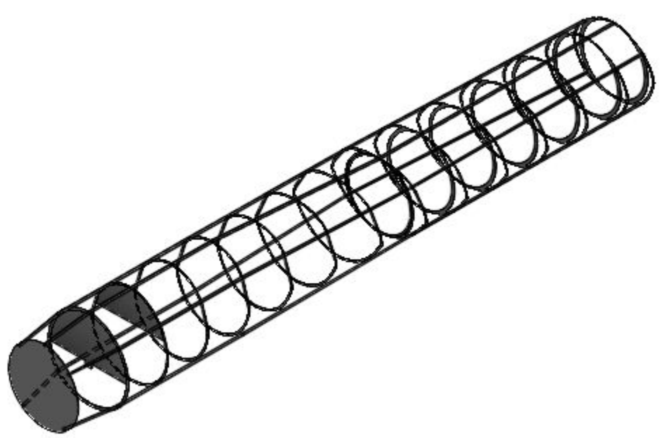

Figure 24. Fuselage Frame

XI. Airfoil Characteristics

A. Overview

The airfoil represents one of the most key aspects when designing an agile and efficient aircraft. When selecting an airfoil for the YFQ-75 we decided to select a modified airfoil which had the thickness to chord ratio to survive repeated carrier landings, had the lift to drag ratio to meet the combat radius for both mission profiles, and be adapted to deal with supersonic travel at speeds of Mach 1 and higher. To meet this goal, we conducted a trade study on the airfoil already employed by the F/A-18 E/F along with several other promising contenders. The results of our research efforts will be documented in the following pages.

B. Thickness-to-Chord Ratio

The thickness-to-chord ratio of an airfoil is critical for determining the wing loading from high gravitational forces and surviving intense carrier landings. That being said, supersonic airfoils generally have a lower thickness-to-chord ratio and the greater the thickness-to-chord ratio, the greater the drag of the aircraft. Thus, the thickness-to-chord ratio must be able to sustain turns of 8.0 degrees per second at 20000 feet while also surviving carrier landings and not having an excessive amount of drag. As with everything when designing an aircraft it is critical to balance these requirements accordingly. In the following sections we will demonstrate how these criteria were balanced and weighted.

C. Lift-to-Drag Ratio

The lift-to-drag ratio of an airfoil is a critical measure of the aircraft's aerodynamic efficiency and is in many ways connected to the thickness-to-chord ratio. Thus these two characteristics must be balanced and optimized when selected an airfoil. For the lift-to-drag ratio, the aerodynamic efficiency of the YFQ-75 directly translates to the combat radius and the fuel efficiency of a plane. A greater lift-to-drag ratio means increased aerodynamic efficiency for the aircraft and is thus preferable for the YFQ-75. For the YFQ-75, more aerodynamic efficiency means having to carry less fuel while also being able to traverse the necessary 700 nautical miles. This is critical to ensure that the airframe has the performance characteristics to meet target objectives and remain a viable mainstay for the Navy.

D. Supersonic Optimization

Commonly airfoils are either optimized for supersonic or subsonic flight. Because the Request for Proposal demands an aircraft which can achieve speeds of Mach 1.6 or higher, the selected airfoil must be capable of supersonic flight and should preferably be optimized for this flight regime. Supersonic optimization is thus a critical requirement for selecting an airfoil and will be weighted heavily in the following decision matrix.

E. Airfoil Contenders

NACA 64A006

Supersonic Optimization: Yes. Has been employed and endured on supersonic vehicles.

Thickness-to-Chord Ratio: 0.06

Lift-to-Drag Ratio: 5.1 @ Mach 1.5

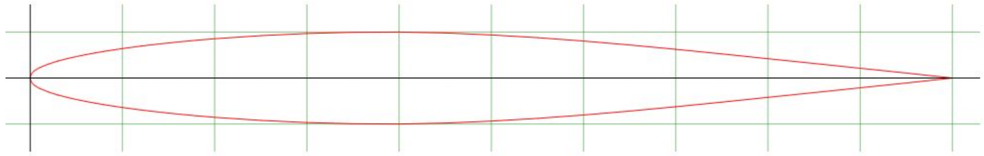

Figure 25: AirfoilTools.com "NACA 64A006 Airfoil Demonstration Model"

NACA 64A204

Supersonic Optimization: Yes. Has been employed and endured on supersonic vehicles.

Thickness-to-Chord Ratio: 0.04

Lift-to-Drag Ratio: 1.8 @ Mach 1.5

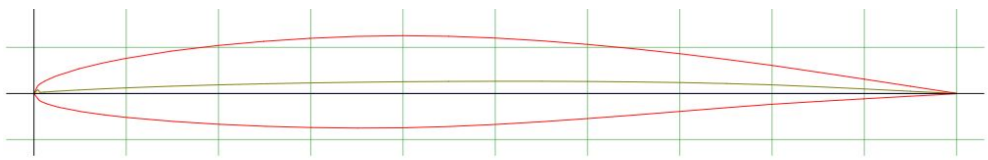

Figure 26: AirfoilTools.com "NACA 64A204 Airfoil Demonstration Model"

NACA 65A005

Supersonic Optimization: Yes. Has been employed and endured on supersonic vehicles.

Thickness-to-Chord Ratio: 0.05

Lift-to-Drag Ratio: 2.1 @ Mach 1.5

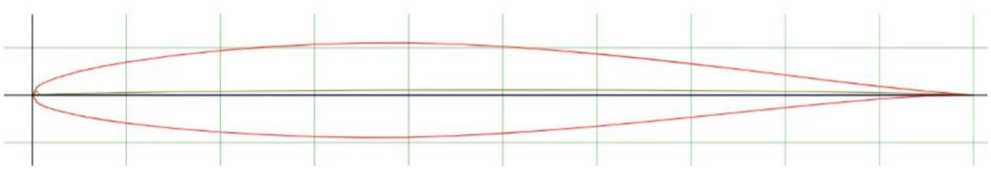

Figure 27: AirfoilTools.com "NACA 65A005 Airfoil Demonstration Model"

F. Airfoil Implementation

Decision Matrix

Here we will explain the weighting system for the decision matrix. There are three main criteria for selecting an airfoil: supersonic optimization, structural integrity, and lift to drag ratio. Each of these criteria were selected for achieving speeds of Mach 1.6, surviving repeated carrier landings, and having the aerodynamic efficiency to have a combat radius of 700 nautical miles. Each of these three criteria is worth 10 points with a proportional weighting for each criteria depending on their respective importance. An airfoil with supersonic optimization has a weight of 0.40 due to its criticality for both the strike and air to air profile, structural integrity has a weight of 0.30 due to its necessity for naval carrier operation, and the lift to drag ratio has a weight of 0.30 to meet the combat radius required from the Request for Proposal.

Airfoil	Supersonic Optimization	Structural Integrity	Combat Radius	Total
64A006	4	3	1	8
64A204	4	1	2	7
65A005	4	2	3	9

G. Final Decision

Ultimately the NACA 65A005 was selected for its proven development and usage on naval systems such as the F/A-18 E/F. While all airfoils surveyed were of a supersonic nature, the NACA 65A005's balance between the lift to drag ratio and the thickness to chord ratio was deemed desirable to sustain carrier operations while also maintaining an adequate combat radius. In future sections of this report, this decision will be further elaborated on, and the design characteristic values of the NACA 65A005 will be implemented in calculations and measurements. Consult the previous slide for information on the characteristics of the NACA 65A005.

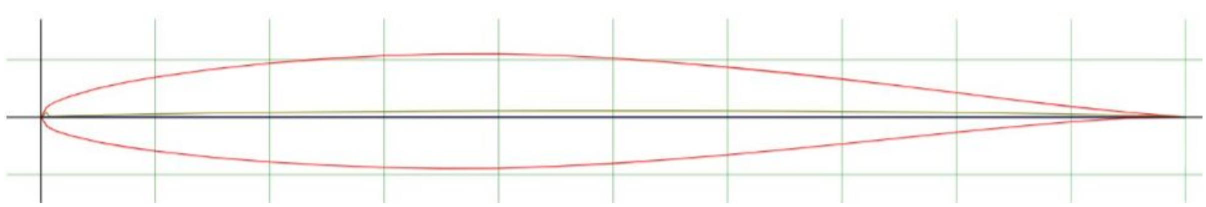

Figure 28: AirfoilTools.com "NACA 65A005 Airfoil Demonstration Model"

XII. Propulsion

A. Engine Selection

The propulsion system selection process involved a comprehensive trade study evaluating multiple engine configurations against mission requirements. The primary candidates considered were single-engine and twin-engine configurations utilizing various turbofan engines suited for high-performance fighter aircraft applications. The F110-GE-132 is the latest member of the GE fighter engine family, fully qualified for operation in the F-16E/F, and was selected by the United Arab Emirates Air Force to power its F-16 Block 60 fleet, entering flight testing in 2003 and production delivery in 2005.[53,63,64] The propulsion system trade study evaluated several advanced engine candidates for the aircraft based on ten weighted criteria.

Criterion	Weight	2 × F119	1 × F135	2 × F414	1 x F110-132	Reasoning / Numbers
Thrust-Weight Ratio	0.33	7.98	6.79	10	8.13	2 x F119: 70,000 lbf / 8900 lb = 7.87; 1 x F135: 43,000 lbf / 6,422 lb = 6.7; 2 x F414: 52,800 / 5,300 = 9.86; 1 x F110-132: 32,500 / 4,050 = 8.02
Cost	0.33	3.03	2.82	5.93	10	2 x F119: $19 mil; 1 x F135: $20.4 mil; 2 x F414: $9.7 mil; 1 x F110-132: $5.75 mil
Weight	0.33	4.55	6.31	8.1	10	2 x F119: ~8,900 lbs; 1 x F135: 6,422 lbs; 2 x F414: ~5,000 lbs; 1 x F110-132: 4,050 lbs
Weighted Totals	1	5.1348	5.2536	7.9299	9.2829	

Figure 25 Engine Decision Matrix

As shown in Figure 25, the F110-GE-132 emerged as the optimal choice, offering the best balance of thrust-to-weight ratio (8.02), lowest cost ($5.75M), and lightest weight (4,050 lbs).[53] The engine produces 32,500 lbf with afterburner and 19,000 lbf intermediate (dry) thrust, exceeding the aircraft's thrust requirements while maintaining excellent operational economics.[53,65] The -132 incorporates a new increased-airflow three-stage long-chord blisk fan derived from the F118 (B-2 bomber), a radial afterburner derived from the F414/F136 family, and a composite outer fan duct, all contributing to improved maintainability and reduced lifecycle cost compared to predecessor variants.[64,65]

B. Inlet, Nacelle, and Exhaust Design

1. Inlet Design and Trade Study

The inlet design must satisfy competing requirements of stealth, pressure recovery, mass flow capability, and integration complexity.[67] A comprehensive trade study evaluated four inlet placement options against weighted criteria covering stealth/RCS, cost, variable-geometry compatibility, pressure recovery, and mass-flow capability.

Criterion (weight)	Weight	Fuselage-Mounted, Rhomboidal	Wing-root / chine	Internal chin / under-fuse	Podded under-wing
Stealth/RCS	0.3	9	8	6	4
Cost / manufacturability	0.2	7	8	7	8
Variable-geometry compat.	0.2	8	7	8	6
Pressure recovery	0.15	8	8	9	7
Mass-flow capability	0.15	8	8	9	7
Weighted total	1	810 (81%)	780 (78%)	750 (75%)	610 (61%)

Figure 26 Intake Decision Matrix

The aircraft employs an adaptive variable-geometry intake system designed to optimize pressure recovery and airflow management across the entire flight envelope. The inlet incorporates internal movable ramps, following a design philosophy similar to that used on the McDonnell Douglas F-15 Eagle and Lockheed Martin F-22 Raptor,[67] allowing the system to dynamically adjust shock positioning and compression ratios as Mach number changes. Variable-geometry ramp designs of this type provide superior high-Mach compression efficiency relative to fixed-geometry alternatives, which suffer reduced pressure recovery at higher Mach numbers due to their reliance on a single detached normal shock.[67]

This configuration provides superior high-Mach compression efficiency while maintaining excellent pressure recovery at both subsonic and supersonic operating conditions. By integrating the variable-geometry components internally, the design preserves low radar cross-section characteristics while still benefiting from advanced inlet flow control capabilities.[59,67] Stealth designs employing serpentine or embedded intakes reduce radar signature at the engine face by blocking the direct line of sight to the compressor stages, which would otherwise produce strong specular reflections.[67]

During takeoff and other low-speed operations, the ramps are positioned to maximize mass flow capture into the engine. In subsonic cruise, the geometry is optimized for efficient pressure recovery and reduced drag, improving overall fuel efficiency. During supersonic flight in the Mach 1.5–2.0 regime, the variable ramps actively manage shock-wave formation and positioning to ensure stable, efficient airflow delivery to the engine face. At high angles of attack, the inlet geometry further adapts to maintain clean and distortion-free airflow into the propulsion system.[67,59]

The intake system is sized around the airflow requirements of the General Electric F110-GE-132 and other comparable F110/F119-class engines.[53] Published datasheet specifications confirm an airflow rate of 275 lb/sec (124.7 kg/sec) and a bypass ratio of 0.68:1.[53,65] The inlet is designed for a peak mass flow rate of approximately 120–140 kg/s per engine at maximum power, with a nominal design point of 130 kg/s for takeoff, sustained high-power operation, and maximum afterburner conditions. During cruise operations, the expected mass flow ranges from roughly 90–115 kg/s depending on throttle setting and altitude. Dimensionally, the intake features an inlet diameter of 123.7 inches to match engine face requirements, while the maximum nacelle diameter reaches 153.3 inches to accommodate the inlet lip, structural members, and internal systems. The total intake length is approximately 262.3 inches, encompassing the intake duct, variable ramp mechanisms, and engine mating interface.[53]

2. Exhaust, Nozzle Selection

The inlet design must satisfy competing requirements of stealth, pressure recovery, mass flow capability, and integration complexity.[67] A comprehensive trade study evaluated four inlet placement options against weighted criteria covering stealth/RCS, cost, variable-geometry compatibility, pressure recovery, and mass-flow capability.

Nozzle	Cost (35%)	RCS (25%)	Mach 2 (20%)	Maintenance Complexity (10%)	Weight (10%)	Final Score
Standard C–D	5	2	4	3	4	3.85
Serrated C–D	4	4	4	4	4	4
Rectangular 2D	1	5	4	1	2	2.65

Figure 27 Nozzle Decision Matrix

The serrated (sawtooth) convergent-divergent variable-area nozzle achieved the highest overall score in the propulsion trade study with a final score of 4.00, outperforming both the conventional C-D and Rectangular 2D configurations across nearly all weighted categories. While the standard C-D nozzle scored marginally higher on raw cost (5 vs. 4), its RCS rating of only 2/5 makes it fundamentally incompatible with the low-observable requirements of a modern stealth fighter platform. The serrated C-D nozzle's sawtooth trailing edge scatters radar returns more effectively, achieving an RCS score of 4/5, while maintaining equivalent supersonic performance at Mach 2. Its modular petal construction also yields improved maintainability over the standard design, scoring 4/5 in that category. As a result, the serrated convergent-divergent nozzle is the selected configuration, providing the best overall balance of stealth performance, supersonic efficiency, cost, and operational sustainability.[68,69]

Compared to more advanced and expensive two-dimensional thrust-vectoring systems, the serrated nozzle offers a far more cost-effective solution while still delivering meaningful survivability improvements. The design also remains maintainable through the use of overlapping feather-style petals constructed from coated titanium alloys and supported by internal air-film cooling systems.[71]

Figure [X] Serrated/Sawtooth Nozzle CAD Model

3. Variable-Area Convergent-Divergent Nozzle

The nozzle itself uses a variable-area convergent-divergent geometry optimized for both subsonic and supersonic operating regimes. The convergent section accelerates exhaust flow to sonic velocity at the throat, while the divergent section further expands and accelerates the flow to supersonic speeds while reducing exhaust pressure toward ambient conditions. Variable throat sizing is critical for maximizing thrust efficiency, especially during afterburner operation when exhaust gas volume increases substantially.[53,62]

To accommodate these changing conditions, a hydraulic or pneumatic actuation system continuously adjusts nozzle area in real time. The serration geometry, implemented as sawtooth or chevron patterns along the petal trailing edges, disrupts organized shock-cell structures within the exhaust plume and enhances turbulent mixing with surrounding air.[68,69] This not only improves IR suppression but also scatters radar energy across multiple directions, reducing specular reflections and overall detectability.[69,70]

Structurally, the nozzle is fabricated from coated titanium alloys selected for their high-temperature resistance and durability under repeated thermal cycling caused by afterburner operation. Internal air-film cooling channels further protect the structure from thermal loads and improve long-term operational reliability.[71]

Figure 28 Convergent-Divergent Nozzle

4. Nacelle Configuration and Integration

The propulsion system is fed by two ventral fuselage-mounted inlets positioned on the lower sides of the forward fuselage, angled outward and downward from the aircraft centerline. This configuration is broadly consistent with inlet arrangements seen on platforms such as the F-35A, where a single ventral inlet feeds the engine from beneath the fuselage, minimizing upper surface disruption and preserving a clean wing-body contour for low-observable shaping. The ventral positioning keeps the inlet faces shielded from forward radar illumination by the fuselage forebody, contributing to reduced frontal RCS. The splitter plates and inlet geometry are designed to divert the turbulent boundary layer airflow away from the engine face, ensuring stable, high-quality airflow delivery to the fan at both subsonic and supersonic conditions. This arrangement also maintains adequate ground clearance during rotation and low-speed operations while allowing maintenance personnel reasonable access at ground level. The nacelle structure has an overall length of approximately 262.3 inches, encompassing the engine core, intake ducting, and accessory sections. The inlet diameter measures 123.7 inches, while the maximum nacelle diameter expands to 153.3 inches around the fan case. At the exhaust section, the nozzle diameter is approximately 119.1 inches, varying with nozzle throat position during operation.[53]

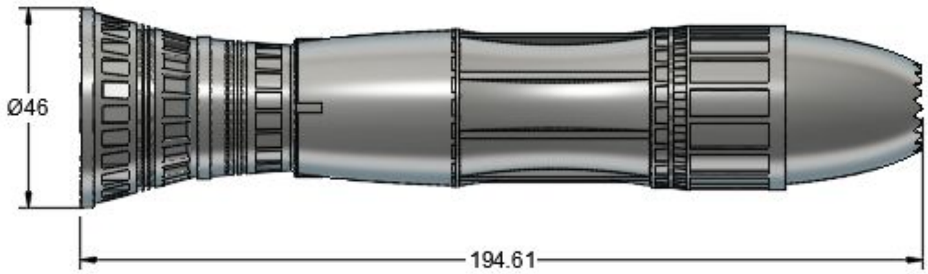

Figure 29 Engine Side View

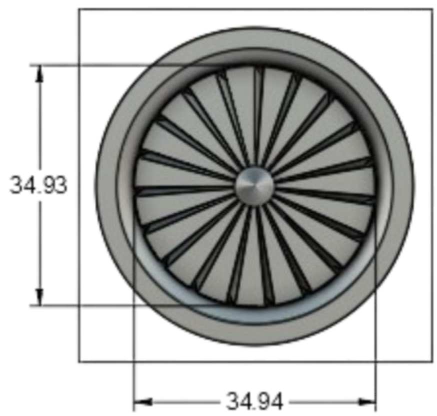

Figure 30 Engine Front View

C. Engine Performance Analysis

The RFP states that a Mach 1.6 dash speed at 30,000 ft is required. To determine whether the F110-GE-132 meets this requirement, a thrust-drag analysis was performed at 30,000 ft across the Mach range from 0.8 to 2.0 under ISA conditions (T = 411.7 °R, ρ = 8.907×10^{-4} slug/ft³, a = 995.0 ft/s). The analysis compares available afterburner thrust against total aircraft drag at a representative mid-mission dash weight of 38,000 lb, using a reference wing area of 400 ft², aspect ratio of 3.5, and Oswald efficiency of 0.80 subsonic / 0.65 supersonic.[53,65] Figure 31 presents the F110-GE-132 afterburner thrust available at 30,000 ft as a function of Mach number. Thrust decreases from sea-level static conditions as altitude reduces air density, but increases above Mach 1.0 as ram pressure recovery partially compensates, peaking at approximately 19,600 lbf near Mach 1.6 before declining at higher Mach numbers.[53,65] The F110-GE-132 datasheet confirms a sea-level static afterburner thrust of 32,500 lbf (144 kN) and an airflow of 275 lb/sec, with the control system automatically increasing airflow and available thrust in response to increasing Mach number signal into the engine control.[65]

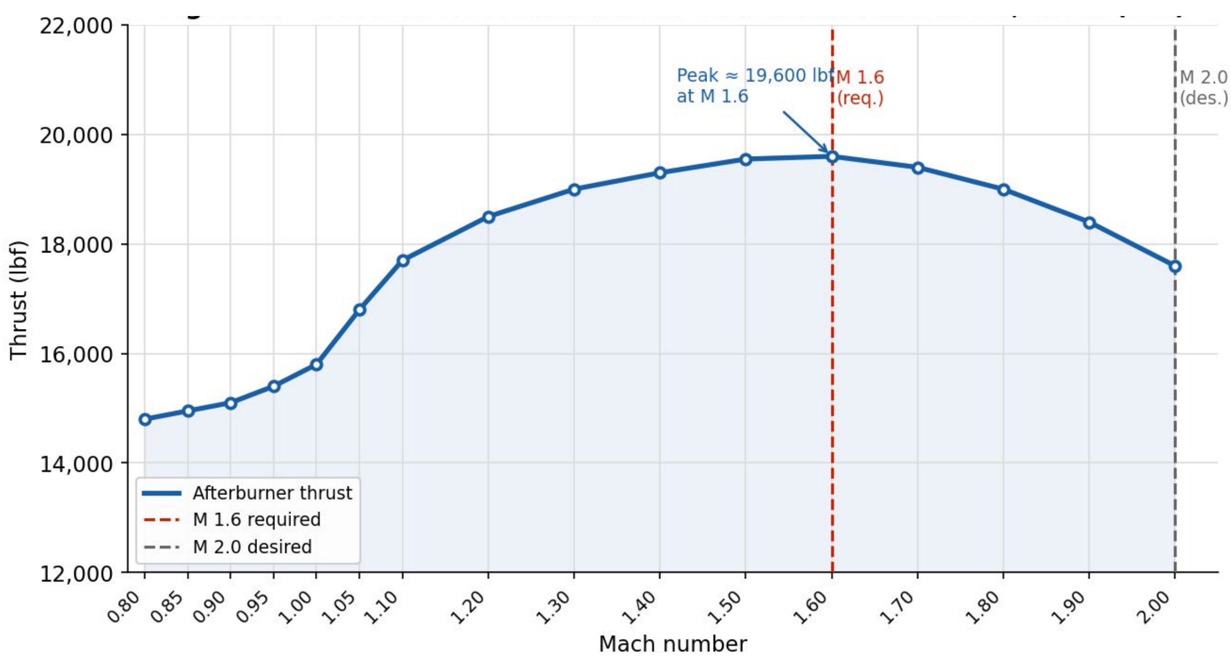

Figure 31 F110-132 Afterburner Thrust @ 30,000 ft (ISA)

Figure 32 presents the total aircraft drag at 30,000 ft across the same Mach range. The drag polar accounts for subsonic parasitic drag (CD0 = 0.018), a transonic drag rise peaking at CD0 = 0.048 near Mach 1.0, and supersonic wave drag reduction thereafter. Despite decreasing CD0 in the supersonic regime, total drag continues to rise above Mach 1.4 as increasing dynamic pressure drives the absolute drag force upward.

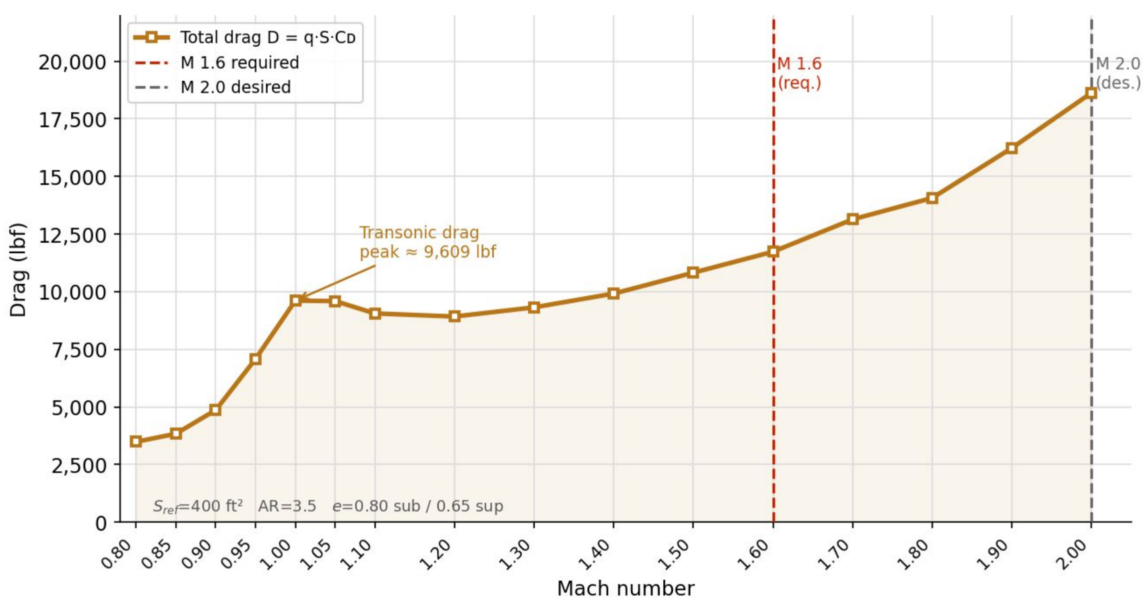

Figure 32 Total Aircraft Drag @ 30,000 ft (ISA)

Figure 33 presents the resulting excess thrust, defined as available afterburner thrust minus total drag, where positive values confirm the aircraft can accelerate or sustain speed in level flight. At Mach 1.6, 30,000 ft, the engine produces approximately 19,600 lbf against a total drag of approximately 11,730 lbf, yielding an excess thrust of +7,870 lbf — a margin of 67% above the drag floor. The required Mach 1.6 dash is therefore met with substantial margin.[53] The desired Mach 2.0 dash speed is not achievable in sustained level flight at this combat weight; at Mach 2.0, drag (~18,630 lbf) marginally exceeds available thrust (~17,600 lbf), resulting in approximately −1,030 lbf excess thrust. Mach 2.0 could be achieved transiently in a slight descent or at a lighter store/fuel state, consistent with the performance envelope of F110-powered aircraft such as the F-16 Block 60/70.[65]

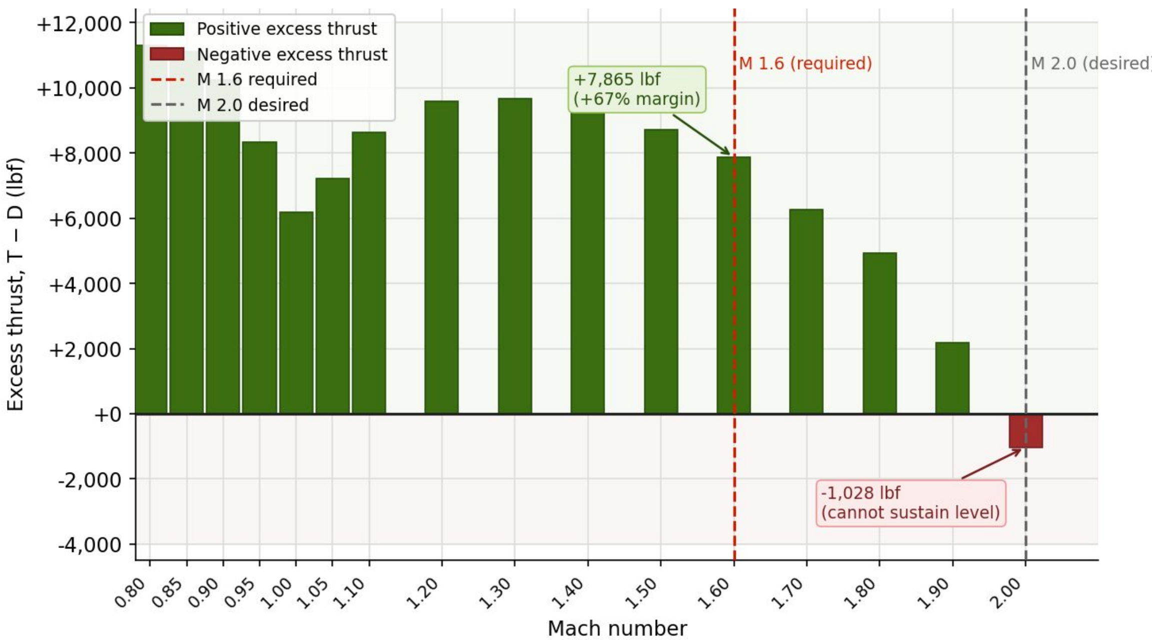

Figure 33 Excess Thrust @ 30,000 ft

XIII. Systems

The YFQ - 75 TRIDENT systems architecture is designed to support high-performance unmanned missions with a focus on versatility. The suite of subsystems, flight control, and electrical power are designed for a wide array of mission scopes - some being to dangerous for a human pilot- and minimal dependence on external support, inspired by proven systems on fighters like the F-18 E/F and X-62 VISTA.

A. Autonomous System

For the full autonomous system, TRIDENT utilizes the main systems for the X-62 VISTA. The X-62 Variable In-Flight Simulation Test Aircraft (VISTA) is an experimental test aircraft used to develop and test autonomous flight and AI-controlled combat systems. The VISTA, a modified F-16D, has demonstrated fully autonomous AI controlled flight and dog-fighting scenarios [38]. The TRL for the VISTA is a 7 as it has a fully functional aircraft that has been flight proven in an autonomous setting. The main systems that provides the VISTA's autonomous capability are the following:

- System for Autonomous Control Simulation (SACS):
  - autonomously control flight
  - autonomously conduct air combat maneuvers
  - perform mission planning and threat response
  - simulate different aircraft flight models
- Enterprise Mission Computer V.2 (EMC2):
  - Core autonomous flight computer
  - Executes AI commands by SACS
  - autonomous flight stabilization
  - AI-driven dog fighting capability
- Galleon Network Attached Storage (NAS):
  - Centralized data storage and processing system
  - mission data processing
  - sensor data aggregation
  - autonomous algorithm updates

Fig 34. VISTA Components [31]

B. Flight Control and Navigation System

Similar to the F/A-18E/F, TRIDENT utilizes a fully digital fly-by-wire flight control system. The system consists of a quadruple-redundant digital flight control architecture operated by four main Flight Control Computers developed by BAE Systems.. Because TRIDENT is fully autonomous, the FCCs do not receive pilot stick, throttle, or rudder pedal inputs. Instead, high-level maneuver commands are generated by the autonomous mission architecture. The SACS autonomy framework determines mission-level flight behavior, while the EMC2 functions as the autonomous flight computer that converts mission objectives into real-time flight commands. These commands are then passed to the FCCs, which execute the control laws, maintain aircraft stability, enforce flight-envelope limits, and command the aircraft actuators.

The FCCs process inputs from the EMC2, inertial measurement unit sensors, air data sensors, angle-of-attack sensors, and control-surface feedback sensors. The FCCs compare these inputs against the commanded flight state and generate actuator commands for the control surfaces. This architecture allows EMC2 to act as the autonomous decision and maneuvering layer, while the FCCs remain responsible for safe, redundant, and stable aircraft control.

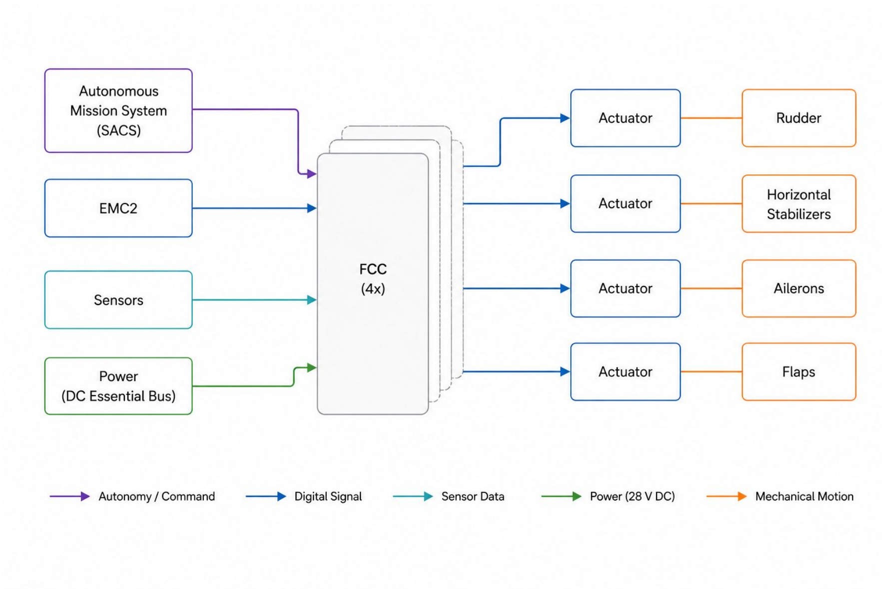

Fig. 35 Diagram of Flight Control System

C. Electric System

TRIDENT's electrical power system is a muli-bus AC/DC architecture designed to ensure continuous power delivery to all onboard systems under both normal and emergency conditions. The system is adapted from modern fighter electrical architectures like the F-18E/F, with modifications to support fully autonomous operation and a single-engine configuration. Primary power is supplied by an engine-driven Integrated Starter-Generator (ISG), which is mechanically coupled to the F100 engine in through the accessory gearbox. During startup, the ISG functions as motor to initiate engine rotation; once the engine is operational, it transitions to generator mode to supply electrical power. The ISG output is regulated by a Generator Control Unit (GCU), which maintains stable voltage and protects against electrical faults.

The generated power is distributed to the Main AC Bus, which supplies high-demand AC systems such as radar and mission systems, as well as non-critical loads. Critical systems are supported by the AC Essential Bus, while an Emergency Bus is maintained to provide power to flight-essential systems during degraded or failure conditions. For DC Power, an AC/DC conversion stage provides power to the DC Main Bus, which supplies non-critical loads. The DC Essential Bus powers critical systems including flight control computers, autonomy processors, navigation sensors, and communication systems. This separation ensures that essential functions are prioritized during abnormal operating conditions.

The aircraft incorporates an onboard battery to provide power prior to engine start and during transient conditions. The battery enables the initial start of avionics, autonomous control systems, and communication systems, and is regulated by a Battery Control Unit (BCU). In the event of primary power loss, the battery supplies short-duration power to essential systems and

Supports the Emergency DC Bus. To ensure survivability during total engine or generator failure, TRIDENT is equipped with a ram air turbine (RAT). The RAT deploys automatically and converts airflow into mechanical energy to drive an emergency generator. This generator supplies power to the Emergency Bus, allowing continued operation of flight-critical systems such as flight control, navigation, and communication systems. Although RAT provides less power than the primary generation, it is sufficient to maintain control and enable recovery.

Redundancy within the electrical system is achieved through the combination of the engine-driven ISG, onboard battery, and RAT-based emergency generator. Additional reliability is provided by AC/DC conversion units, automatic bus switching, and load shedding logic that prioritizes essential systems during failure conditions. This layered power architecture ensures that TRIDENT maintains autonomous flight capability across all mission phases, including startup, normal operation, and emergency scenarios. An overview of the electrical system is shown in Fig. 36.

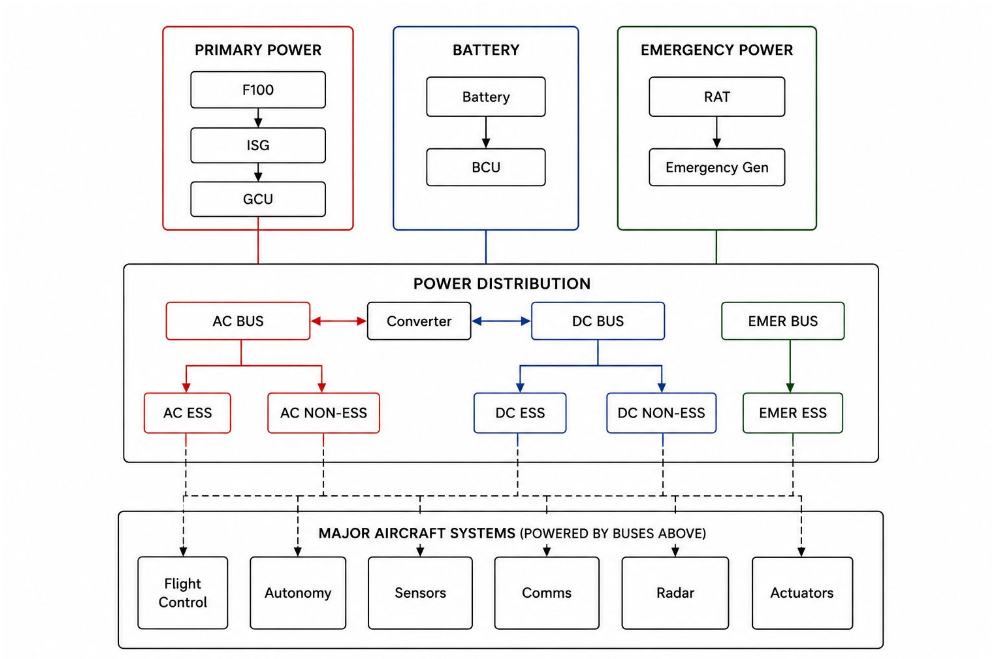

Fig. 36 Diagram of Electrical System Architecture

D. Hydraulic System

The hydraulic system onboard TRIDENT is based on modern carrier-capable fighter architectures, with modifications to support a single-engine configuration and fully autonomous operation. The hydraulic system provides flow to control surface actuators, the landing gear system, brakes, and steering systems.

The hydraulic system is divided into two independent subsystems: System A and System B. Each system is equipped with an engine-drive hydraulic pump as its primary source of pressure. In addition, both systems incorporate a backup electric hydraulic pump powered by the onboard electrical system. In the event of engine failure, emergency power is supplied by the

RAT, which enables continued operation of the electric hydraulic pumps. The hydraulic architecture is simplified compared to legacy twin-engine systems due to the use of an integrated starter-generator for engine start, eliminating the need for a hydraulic jet fuel starter.

For increased survivability and redundancy, both System A and System B supply hydraulic flow to critical flight control surfaces, landing gear, and braking systems. This dual-supply architecture ensures that loss of a single hydraulic subsystem does not result in loss of control authority. Non-critical systems are distributed between the two subsystems to reduce load and improve fault isolation.

In the event of engine or primary pump failure, at least one hydraulic subsystem remains operational through RAT-supported electric pumps, allowing TRIDENT to maintain sufficient flight control authority for recovery and landing operation. This redundant hydraulic architecture ensures continued autonomous flight capability under degraded conditions.

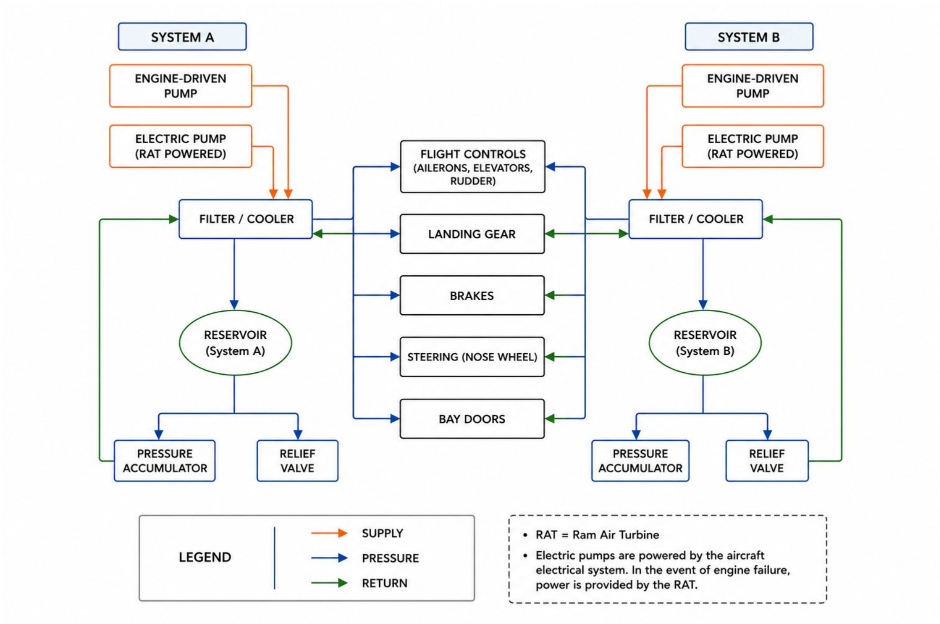

Fig. 37 Diagram of Hydraulic System Architecture

XIV. Avionics

The aircraft's fully autonomous design requires extensive avionics integration and system redundancy. Without a pilot onboard, all situational awareness, decision-making, and flight control functions must be performed by onboard systems. To address this, TRIDENT incorporates a layered avionics architecture consisting of autonomy, sensing, and networking subsystems that enable real-time decision-making and control. This architecture emphasizes redundancy and fault tolerance to maintain survivability in contested environments. Fig. 38 details the onboard avionics architecture that enables all mission operations for TRIDENT.

Fig. 38 Onboard Electronics Suite

Component	Primary Role	Volume (ft^3)	Weight (lb)
X-62 VISTA SACS	Autonomous flight control and AI mission management	N/A	N/A
EMC2	Autonomous mission control and decision-making	1.7	90
Galleon NAS	Onboard AI data storage and processing	0.2	8
AN/APG-79 Radar	Long-range air dominance radar	26.0	500
AN/ALQ-214 IDECM	Electronic warfare and missile defense	3.8	285
DTP-N	Distributed targeting and sensor fusion	0.6	41
MIDS-LVT(1)	Tactical data link and network communications	0.6	42
AN/ASQ-228 ATFLIR	Passive precision targeting for autonomous strike operations	5.2	420

The avionics architecture is organized into four primary functional subsystems: autonomous control, sensing, electronic warfare, and networked communication. These subsystems work together to create a fully integrated, network-centric combat aircraft capable of operating with minimal human intervention.

A. Autonomous Control Subsystem

The autonomous control subsystem consists of the X-62 VISTA System for Autonomous Control Simulation (SACS), EMC2, and the Galleon Network Attached Storage (NAS). SACS provides the core autonomy framework, enabling mission planning, threat response, and AI-driven flight behavior. EMC2 functions as the real-time autonomous flight computer, executing control laws and maneuver commands while interfacing with the flight control computers. The Galleon NAS supports onboard data storage, sensor data aggregation, and AI model management, allowing continuous adaptation and improvement of autonomous algorithms.

Fig. 39 Radar Selection Trade Study

	APG-79 (F/A-18E/F)	APG-77 (F-22)	APG-63(V)3 (F-15)
1. Radar Architecture & Technology			
Radar Type	AESA	AESA	AESA
Antenna Steering	Fully Electronic	Fully Electronic	Fully Electronic
T/R Module Tech	GaN AESA	AESA Tile-based	AESA (GaAs/Hybrid)
Frequency Band	X-Band	X-Band	X-Band
Design Driver	Maritime, Multi-role	Stealth, Air Dominance	F-15 Upgrade
2. Detection, Tracking & Engagement			
LPI / LPD	High	Very High	High
Frequency Agility	Very High	Very High	High
Adaptive Beamforming	Advanced	Advanced	Moderate–High
Jamming Resistance	High	Very High	High
3. Survivability & Electronic Warfare			
LPI / LPD	High	Very High	High
Frequency Agility	Very High	Very High	High
Adaptive Beamforming	Advanced	Advanced	Moderate–High
Jamming Resistance	High	Very High	High
4. Reliability, Maintainability & Availability			
Architecture	Distributed	Distributed	Distributed
Maintenance Burden	Low–Moderate	Low	Low–Moderate
Support Infrastructure	High (Navy fleet, in service)	Moderate (limited fleet)	Very High (global fleet)
5. Cost, Risk & Programmatic Factors			
Unit Cost	$6.5–7.5M	$7–7.5M	$5–6M
Production Status	In production	Limited / legacy	Low-rate production
Program Risk	Low	Medium–High	Low
Exportability	Restricted	Highly restricted	Exportable
Carrier Proven	Yes	No	No
6. Trade Study Scoring (1-5)			
Carrier Suitability	5	2	2
Low Observability (LPI)	4	5	3
Detection Capability	4	5	3
Multimode Capability	4	5	2
Affordability	3	2	5
Integration Risk	5	2	4
Reliability & Support	5	2	4

Criterion	Weight	APG-79 (F/A-18E/F)	APG-77 (F-22)	APG-63(V)3 (F-15)
Carrier Suitability	0.2	1	0.4	0.4
Integration Risk	0.18	0.72	0.9	0.54
Reliability & Support	0.15	0.6	0.75	0.45
Detection Capability	0.12	0.48	0.6	0.24
Low Observability (LPI)	0.1	0.3	0.2	0.5
Multimode Capability	0.1	0.5	0.2	0.4
Affordability	0.15	0.75	0.3	0.6
TOTAL	1	4.35	3.35	3.13

B. Sensing Subsystem

The sensing subsystem is centered around the AN/APG-79 AESA Radar and AN/ASQ-228 Advanced Targeting Forward-Looking Infrared (ATFLIR). A radar trade study was conducted comparing the APG-79, APG-77, and APG-63(V)3 across key criteria including carrier suitability, integration risk, reliability and support, detection capability, low observability (LPI), multimode capability, and affordability [26] [27] [28]. Each category was assigned a weighting based on its importance to TRIDENT's mission as a carrier-based, fully autonomous combat aircraft. Carrier suitability was assigned the highest weighting (0.20), because TRIDENT is designed to replace the F/A-18E/F and must reliably operate in maritime environments, including catapult launches, arrested landings, and exposure to saltwater conditions. Integration risk was also heavily weighted (0.18), as the autonomous architecture requires seamless compatibility between the radar and onboard systems such as EMC2 and DTP-N. Minimizing integration complexity reduces development risk and improves system reliability.

Reliability and support (0.15) and affordability (0.15) were emphasized to ensure long-term operational sustainability and cost-effectiveness, particularly given the intent for scalable production and development. Detection capability (0.12) and low observability performance (0.10) were weighted slightly lower, as all candidate systems already provide high-end performance in these areas, making them less influencing factors. Multimode capability (0.10) was included to account for the need to support multiple mission profiles, including air-to-air, air-to-ground, and maritime operations.

Based on this weighted evaluation, the APG-79 achieved the highest total score of 4.35, compared to 3.35 for the APG-77 and 3.13 for the APG-63(V)3. While the APG-77 demonstrated superior stealth and detection performance, its limited production status and integration challenges reduced its overall suitability. The APG-63(V)3 offered strong affordability and supportability but lacked optimization for carrier-based operations. The APG-79 provides the best balance of performance, integration, and operational compatibility for TRIDENT.

The AN/APG-79 enables long-range detection, multi-target tracking, and low probability of intercept operation, supporting autonomous situational awareness and beyond-visual-range engagement. The AN/ASQ-228 ATFLIR targeting pod complements the radar by providing passive infrared sensing, electro-optical imaging, and precision targeting capability [29]. This allows TRIDENT to perform autonomous strike operations and maintain sensor redundancy in contested environments. Together, these systems ensure robust detection, tracking, and engagement capability across all mission profiles.

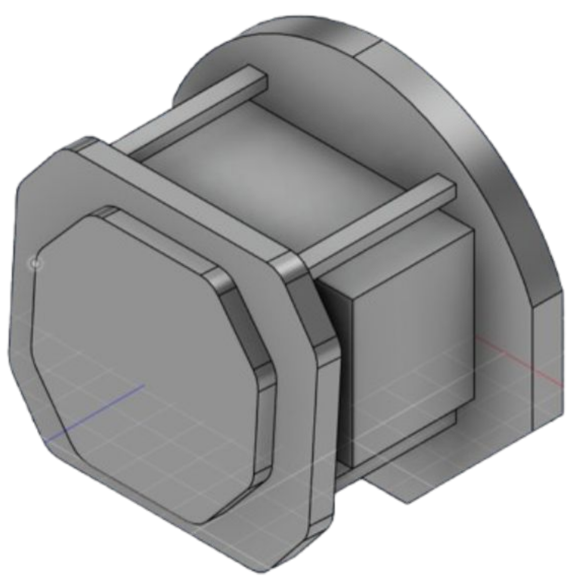

Fig. 40 CAD Model of APG-79

C. Electronic Warfare Subsystem

The electronic warfare and network/communication subsystems for TRIDENT are directly derived from the F/A-18E/F architecture, utilizing the AN/ALQ-214 Integrated Defensive Electronic Countermeasures (IDECM) system and the MIDS-LVT(1) tactical datalink. This design decision aligns with TRIDENT's core tenets of detectability, survivability, and lethality, while also prioritizing affordability and minimizing integration risk through the use of proven, in-service systems.

From a survivability and detectability standpoint, the AN/ALQ-214 IDECM system provides the primary layer of active electronic warfare protection for TRIDENT. THe system protects the aircraft by continuously monitoring the electromagnetic environment to detect, identify, and classify hostile radar emissions, including search, track, and missile guidance radars. Once a threat is identified, the ALQ-214 employs digital radio frequency memory (DRFM)-based jamming techniques to generate deceptive signals that mislead enemy radar systems [36]. Rather than simply blocking radar signals, the system creates false targets, alters the apparent position and velocity of the aircraft, and disrupts missile guidance solutions. This significantly reduces the probability of successful target tracking and missile interceptions. In the case of radar-guided missile threats, the ALQ-214 works in conjunction with onboard countermeasures to degrade or break the missile's lock, effectively increasing the aircraft's survivability without requiring pilot input.

Additionally, the system operates automatically and in real time, which is critical for a fully autonomous platform. By integrating threat detection, electronic attack, and countermeasure deployment into a single system, the ALQ-214 reduces pilot workload in traditional aircraft and enables TRIDENT to independently respond to complex threat environments. This capability directly supports the aircraft's survivability by allowing it to avoid, confuse, or defeat incoming threats, while also contributing to reduced detectability by limiting the effectiveness of enemy radar systems.

D. Network and Communication Subsystem

The network and communication subsystem, consisting of the MIDS-LVT(1) datalink and the Distributed Targeting Processor - Networked (DTP-N), directly enhances TRIDENT's lethality. The MIDS-LVT enables secure Link-16 communication, allowing the aircraft to share and receive targeting data in real time with other aircraft and carrier strike group assets [33]. The DTP-N performs sensor fusion, integrating radar, electronic warfare, and external datalink inputs into a unified tactical picture [32]. This enables cooperative targeting, beyond-visual-range engagement, and coordinated strike operations, significantly increasing mission effectiveness.

By retaining these subsystems from the F/A-18E/F, TRIDENT achieves a balanced design that supports all three core tenets. Detectability is reduced through active electronic warfare, survivability is enhanced through proven defensive systems, and lethality is increased through networked targeting and data sharing. At the same time, leveraging existing government-furnished equipment reduces development cost, lowers integration complexity, and ensures compatibility with current naval infrastructure.

XV. Ordinance

The TRIDENT ordnance configuration is designed to provide a balance between lethality, flexibility, and cost-effectiveness while supporting both air-to-air and air-to-ground mission profiles. Unlike stealth-focused aircraft that rely on internal weapons bays, TRIDENT utilizes an external pylon configuration to simplify design, reduce structural complexity, and increase payload flexibility. This approach aligns with the program's core tenets by maximizing lethality and affordability while accepting a trade-off in detectiblity. The aircraft is equipped with four external wing pylons, consisting of two inner pylons and two outer pylons, as well a wingtip stations. This configuration allows TRIDENT to carry a wide range of ordnance while maintaining compatibility with existing U.S. Navy weapon systems.

A. Air-to-Air Configuration

The air-to-air configuration is optimized for beyond-visual-range (BVR) engagement and close-range dogfighting capability. The primary weapon employed is the AIM-120 AMRAAM, supported by AIM-9X missiles for short-range engagements. The inner pylons utilize BRU-32 ejector racks paired with LAU-127 rail launchers, allowing each station to carry two AIM-120 missiles. The outer pylons are equipped with LAU-127 rail launchers, each carrying one AIM-120 missile. Wingtip stations are also fitted with LAU-127 rail launchers, each carrying one AIM-9X missile.

This configuration results in a total loadout of:

- 6 x AIM-120 AMRAAM
- 2 x AIM-9X

This loadout maximizes air-to-air lethality by enabling multiple simultaneous engagements while maintaining high maneuverability and minimal system complexity.

B. Air-to-Ground Configuration

The air-to-ground configuration is designed for precision strike missions while retaining limited self-defense capability. The primary strike weapon is the MK-83 Joint Direct Attack Munition (JDAM), providing all-weather, GPS-guided precision targeting. Both inner and outer pylons are equipped with BRU-32 ejector racks, each carrying one MK-83 JDAM. Wingtip stations retain AIM-9X missiles for defensive purposes against airborne threats. A centerline-mounted AN/ASQ-228 ATFLIR targeting pod is included to provide precision targeting, infrared imaging, and electro-optical tracking capability. This enables accurate target identification and engagement in both day and night operations.

This configuration results in a total loadout of:

- 4 x MK-83 JDAM
- 2 x AIM-9X
- 1 x ATFLIR Targeting Pod

C. Capability and Design Rationale

The external ordnance configuration provides TRIDENT with a highly flexible and modular weapons system capable of supporting multiple mission profiles without requiring significant structural or mechanical complexity. By leveraging existing launch systems such as the BRU-32 and LAU-127, the design minimizes integration risk and reduces overall program cost. While the use of external pylons increase radar cross section compared to internal carriage, this trade-off is mitigated through the use of electronic warfare systems and mission planning. This approach aligns with TRIDENT's design philosophy of balancing cost and capability, prioritizing lethality and affordability while maintaining acceptable levels of survivability and detectability.

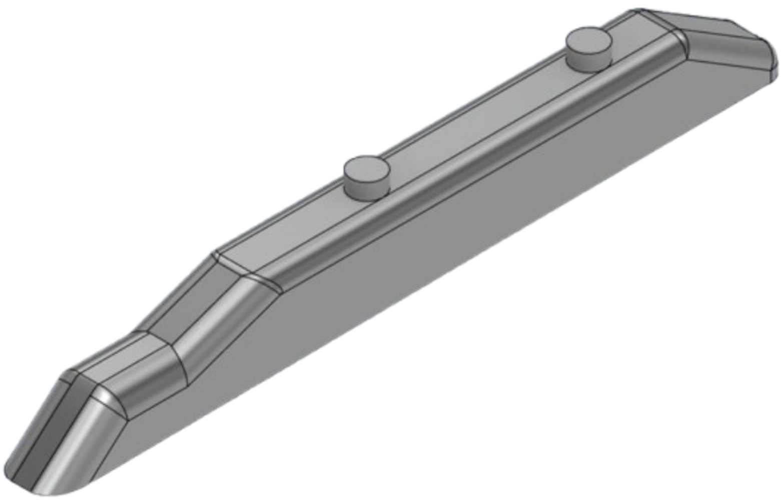

Fig. 41 CAD Model of Outer Pylon

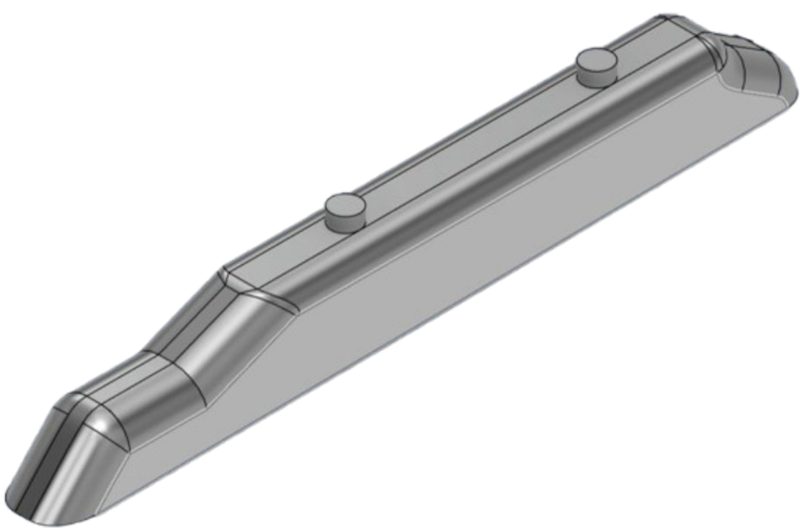

Fig. 42 CAD Model of Inner Pylon

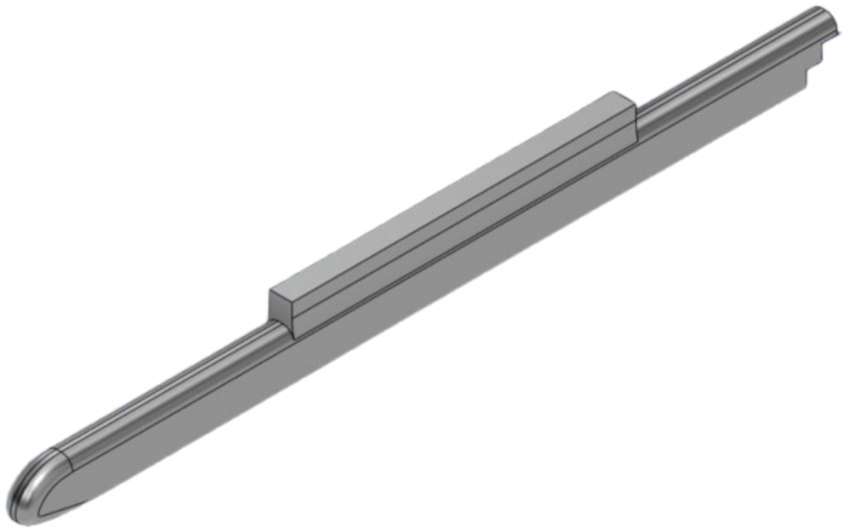

Fig. 43 CAD Model of LAU-127 Rail Launcher

XVI. Landing Gear

A. Landing Gear Configuration

The landing gear system for TRIDENT is based on the F/A-18E/F landing gear architecture due to its proven carrier suitability and ability to withstand high-load carrier recovery conditions. Since TRIDENT is designed as a carrier-based replacement for the F/A-18E/F, adopting similar landing gear arrangement reduces development risk while ensuring compatibility with catapult launch, arrested recovery, and deck handling requirements. This follows the goal of using proven systems where possible to balance cost, capability, and integration risk. The RFP emphasizes that the aircraft must be compatible with existing CVN-68 and CVN-78 carriers and carrier equipment, making carrier-suitable landing gear a critical design driver.

TRIDENT utilizes a tricycle landing gear configuration consisting of one nose landing gear assembly and two main landing gear assemblies. This configuration was selected based on the F/A-18E/F arrangement because it provides stable ground handling, effective braking distribution, and compatibility with carrier deck operations. In a tricycle arrangement, the main landing gear are located behind the aircraft center of gravity while the nose is located forward of it, keeping the aircraft stable and during landing. Raymer notes that this arrangement allows aircraft to land at relatively large crab angles, which is beneficial for carrier recovery where crosswinds, deck motion, and rapid deceleration may occur (Raymers, 354).

Fig 44. CAD Model of Landing Gears Retracted Out

B. Landing Gear Loads and Sizing

Gear loads were determined through moment balancing using the aircraft's center of gravity and landing gear locations, while tire and oleo sizing followed Raymer's landing gear methodology. For TRIDENT, the datum was defined at the nose of the aircraft, with the x-axis running aft along the fuselage, the y-axis running laterally across the wing, and the z-axis running vertically. The current landing weight use for the landing gear sizing was 33,814.37lb. The aircraft center of gravity was located at about 25ft from the nose, the nose gear was located at 13.730ft, and the main landing gear was located at 29.363ft from the nose. Using static force and moment equilibrium, the expected nose landing gear load was calculated to be 13,263.52lb, while the total main landing gear load was calculated to be 20,550.85lb, or 10,275.42lb per main gear. The placement of the gears in the tricycle layout was selected so that the main gear accounts for 61% of the load upon landing, with the nose gear accounting for 39%.

The selected tires were based on F/A-18E/F tire sizing and verified using Goodyear tire data. The nose landing gear uses 22 x 6.6 -10in tire with a rated load of 14,150lb, a rated braking load of 21,225lb, and a rated speed of 240 mph. The main landing gear uses a 32 x 11.5 - 15in tire with a rated load of 27,800lb, a rated braking load of 41,700lb, and a rated speed of 242 mph. The expected static loads were compared to rated tire loads to confirm that the selected tires provide sufficient load capacity for the current aircraft configuration.

Raymer's methodology was also used to guide shock absorber sizing. For high-performance naval aircraft, Raymer lists Navy fighter landing gear load factors in the range of 5.0-6.0, reflecting severe landing loads associated with carrier operations. Raymer also states that oleo shock absorber diameter is determined by the load carried by the oleo and that a typical oleo internal pressure is approximately 1800 psi (Raymers, 368). Therefore, an oleo pressure of 1800 psi was used as the baseline value for the TRIDENT landing gear sizing table.

Aermet 100 was chosen for TRIDENT's landing gear because it is already used in major structural parts of the F/A-18E/F landing gear, making it a proven material for carrier aircraft. Since our nose and main landing gear were based on the F/A-18E/F, using the same material helps keep the design realistic and reduces risk. The landing gear has to handle repeated carrier landings, catapult launches, braking loads, and arrested recoveries, so the material needs to be very strong while also resisting fatigue and crack growth. Aermet 100 fits this requirement because it has a yield strength of about 1620-1725 MPa. For this reason, it was selected for the main structural parts of the nose gear, main gear, launch bar support, and arresting hook attachment areas.

Fig. 45 Landing Gear Specifications

Parameter	Main Gear (1x)	Nose Gear
X Location (ft)	29.363	13.730
Y Location (ft)	±4.004	0
Z Location (ft)	-4.3	-4.3
Tire Diameter (in)	32	22
Tire Width (in)	11.5	6.6
Wheel Rim Diameter (in)	15	10
Expected Max Load (lb)	10,275.42	13,263.52
Rated Load (lb)	27,800	14,150
Rated Braking Load (lb)	41,700	21,225
Rated Tire Speed (mph)	242	240
Oleo Pressure (psi)	1,800	1,800

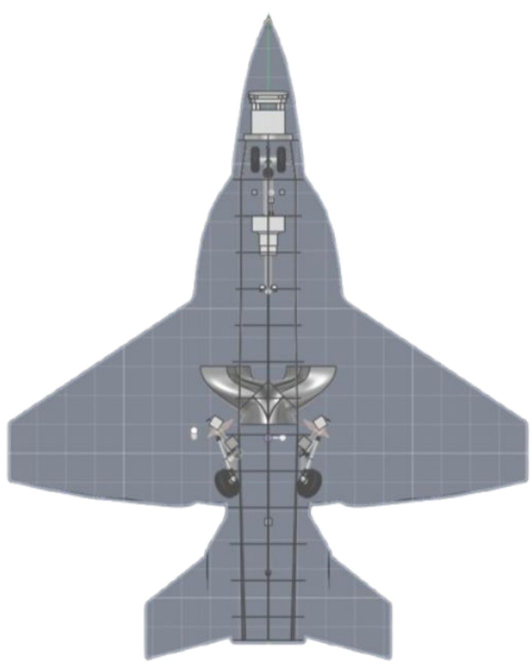

Fig 46. Landing Gear Stowed View

C. Nose Landing Gear and Launch Bar

The nose landing gear assembly for TRIDENT was modeled after the F/A-18E/F nose gear due to its proven compatibility with carrier catapult launch and arrested recovery operations. As shown in Fig. 47, the assembly uses a dual-wheel nose gear arrangement with a central shock strut, upper mounting structure, hydraulic retraction linkage, and catapult launch bar. The dual-wheel configuration improves load distribution during carrier deck operations and provides additional stability during taxi, launch, and recovery.

The central shock strut is the primary load-carrying member of the nose gear assembly. It absorbs vertical loads during landing and supports the forward fuselage during ground operations. The upper mounting structure connects the gear to the aircraft frame and provides the structural interface for retraction and deployment. The retraction linkage allows the nose gear to rotate into the fuselage during flight, reducing drag and protecting the assembly from the external flow field.

A key feature of the nose landing gear is the catapult launch bar mounted near the lower forward portion of the assembly. This launch bar allows TRIDENT to interface with the aircraft carrier catapult shuttle during launch. During catapult operations, the launch bar transfers the forward pulling force from the catapult system into the nose gear structure, accelerating the aircraft to takeoff speed within the limited deck length. Because of this role, the launch bar is one of the most structurally critical components of the nose landing gear.

Finite element analysis was conducted on the TRIDENT catapult launch bar to evaluate its structural response under launch loading. The maximum directional deformation was 20.713 mm, occurring near the free end of the launch bar. This behavior is expected because the launch bar acts similarly to a cantilevered member during catapult loading. The maximum equivalent elastic strain was 0.016524 mm/mm, while the maximum von Mises stress was 1184.1 MPa. Both the strain and stress concentrations occurred near the launch bar root and attachment region, indicating that this area is the primary structural load path and should be reinforced in future design iterations.

Overall, the TRIDENT nose landing gear design provides carrier launch compatibility, stable ground handling, and realistic packaging within the forward fuselage. This inclusion and analysis of the launch bar demonstrates that the nose gear was designed not only for landing support, but also for the specific requirements of carrier-based aircraft operations.

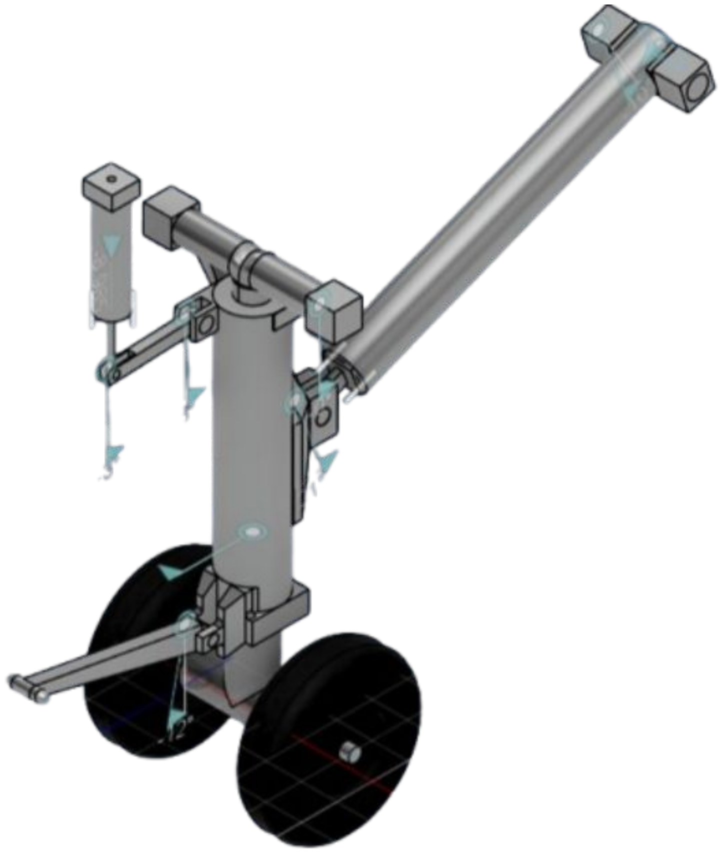

Fig 47. CAD Model of Nose Landing Gear

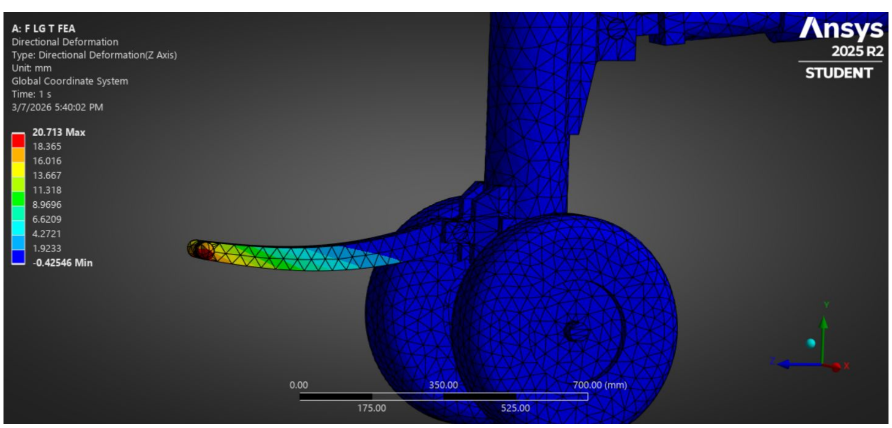

Fig 48. Directional Deformation FEA

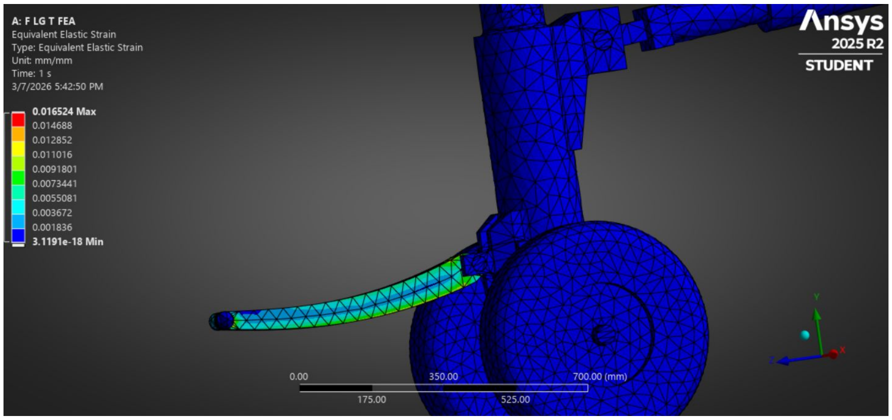

Fig 49. Equivalent Elastic Strain FEA

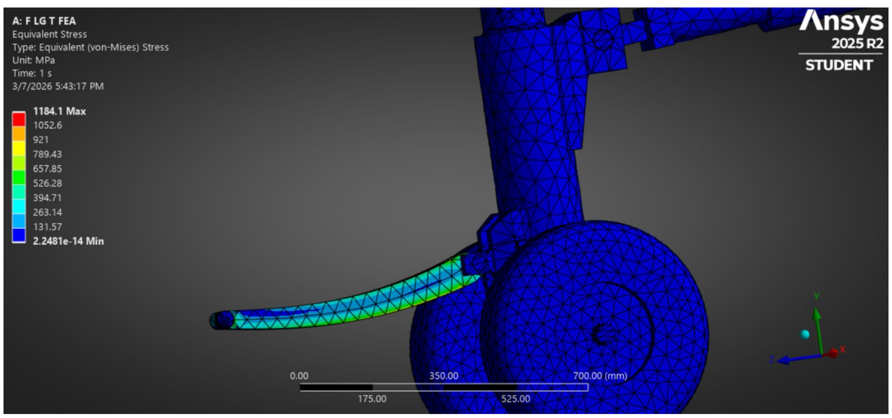

Fig 50. Equivalent (von-Mises) Stress FEA

Analysis Type	**Result Measured**	**Minimum Value**	**Maximum Value**	**Location of Maximum Response**
Directional Deformation	Z-Axis Displacement	-0.425mm	20.713mm	Free end of launch bar
Equivalent Elastic Strain	Elastic Strain	3.119 x 10^{-18}mm/mm	0.016524 mm/mm	Near launch bar root
Equivalent von Mises Stress	Combined Stress	2.248 x 10^{-14}MPa	1184.1 MPa	Near launch bar root

Fig. 51 Catapult Launch Bar FEA Results

D. Main Landing Gear and Arresting Hook

The TRIDENT main landing gear was modeled after the F/A-18E/F main landing gear to support the high-load requirements of carrier recovery. Unlike conventional runway-based aircraft, carrier-based aircraft experience high sink-rate landings, rapid arrestment loads, and compact deck handling constraints. For this reason, the main landing gear was designed with a robust shock strut, angled support linkage, and a retraction mechanism inspired by the F/A-18E/F architecture.

As shown in Fig. 52 and 53, each main landing gear assembly uses a single-wheel configuration attached to a primary oleo shock strut. The shock strut acts as the main load-absorbing member during touchdown, reducing impact loads transmitted into the fuselage and wing-root structure. The side brace and retraction linkage provide lateral stability and guide the motion of the gear during deployment and stowage. This arrangement allows the gear to fold into the aircraft while maintaining its structural integrity to withstand carrier loads.

The main landing gear is positioned behind TRIDENT's aircraft center of gravity, consistent with the tricycle landing gear configuration. This placement provides ground stability, supports braking loads, and helps prevent nose-over during landing and deck operations. Since TRIDENT is fully autonomous, stable and predictable ground handling is important because taxi, launch, and recovery operations rely on automated control logic rather than direct pilot input.

Just like the catapult launch bar, TRIDENT also incorporates an arresting hook system to enable carrier landings. Since the aircraft is designed to replace the F/A-18E/F in a carrier-based role, the ability to perform arrested landings is a required feature. The arresting hook is mounted along along the lower rear of the fuselage and extends downward during recovery to engage the carrier arresting wire. Once engaged, the hook transfers the aircraft's forward kinetic energy into the ship's arresting gear system, allowing TRIDENT to rapidly decelerate within the limited runway distance available on an aircraft carrier.

The arresting hook was modeled as a long structural arm with a reinforced forward mounting bracket and a hook interface at the bottom end. The forward bracket provides the primary structural attachment point to the fuselage and must be capable of carrying the large tensile and bending loads generated during arrested recovery. The hook end is shaped to capture the deck cable and maintain engagement during deceleration.

Overall, the main landing gear and arresting hook were designed to ensure TRIDENT can safely operate in the demanding carrier environment. By basing these systems on the proven F/A-18E/F configuration, TRIDENT benefits from an established naval aircraft layout capable of handling high sink-rate landings, arrested recoveries, and compact deck operations. The main landing gear provides the structural support and shock absorption required during touchdown, while the arresting hook enables rapid deceleration during carrier recovery. Together, these systems strengthen TRIDENT's carrier suitability, reduce development risk, and support the overall design goal of creating a cost-effective unmanned replacement for the F/A-18E/F.

Fig. 52 CAD Model of Left Main Landing Gear

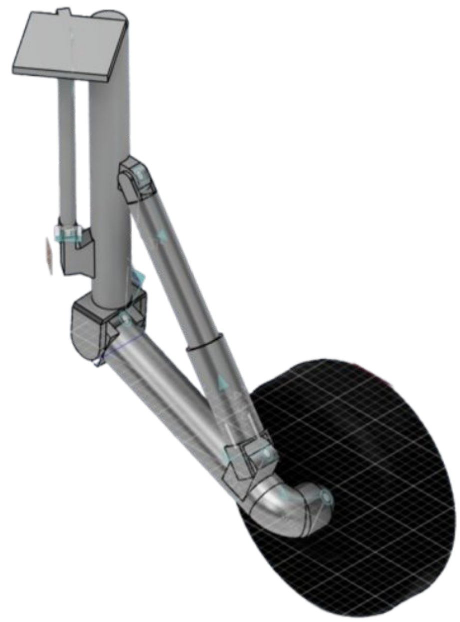

Fig. 53 CAD Model of Right Main Landing Gear

Fig 54. CAD Model of Arresting Hook

XVII. Performance

This section details the performance evaluation of the YFQ-75 TRIDENT aircraft. To ensure compliance with the RFP, the TRIDENT's performance calculations were iterated throughout the design process. The performance criterias evaluated are takeoff and landing speed, dash speeds at sea level and at 30,000 feet, sustained turn rate and combat radius. The subsequent sections discuss in detail the team's findings regarding the YFQ-75 TRIDENTs' performance metrics.

A. Mission Profiles

The TRIDENT has been designed to be superior in two mission sets, Air to Ground strikes and Air to Air Combat. The following figures establish the operational conditions the aircraft is expected to operate under, this includes phases such as takeoff , target engagement, loitering and recovery aboard a CVN 68/78 carrier. These profiles serve as a baseline for assessing the aircrafts efficiency and RFP compliance.

Mission Phase	Description	Performance
1-2'	Takeoff from CV68/78 carrier	-
2-3'	Climb	Ascend to 30,000 ft cruise until target
3-4'	Descend to target dash (25 nm)	Dash at mach 0.9 during ingress
4-5'	Engage Target	-
5-6'	Egress dash (25 nm)	Dash at mach 0.9 during egress
6-7'	Climb	Ascend to 30,000 ft cruise until carrier
7-8'	Descend to carrier	-
8-9'	Loiter	10,000 feet loiter
9-10'	Land on CV68/78	Land at approx airspeed of 145 knots

Figure 55: Ground Strike Mission Profile Chart

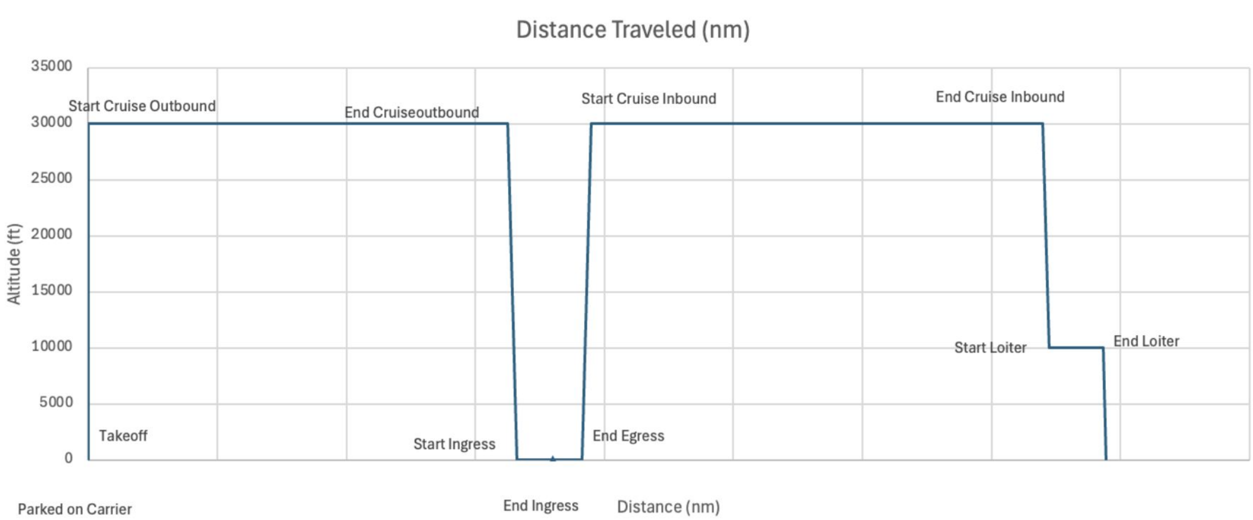

Figure 56 : Ground Strike Flight Profile

Mission Phase	Description	Performance
1-2'	Takeoff from CV68/78 carrier	-
2-3'	Climb	Ascend to 30,000 ft cruise until target
3-4'	Supersonic Dash	1.6-2.0 mach at 30,000 feet
4-5'	Descend for combat manuvers	2 mins of afterburner at 10,000 ft
5-6'	Climb	Ascend to 30,000 ft cruise
6-7'	Descent towards carrier	-
7-8'	Loiter	20 minutes at 10,000 ft
8-9'	Land on CVN68/78 carrier	Approach speed below than 145 knots

Figure 57: Air to Air Mission Profile Chart

Figure 58 : Air to Air Flight Profile

B. Flight Envelope

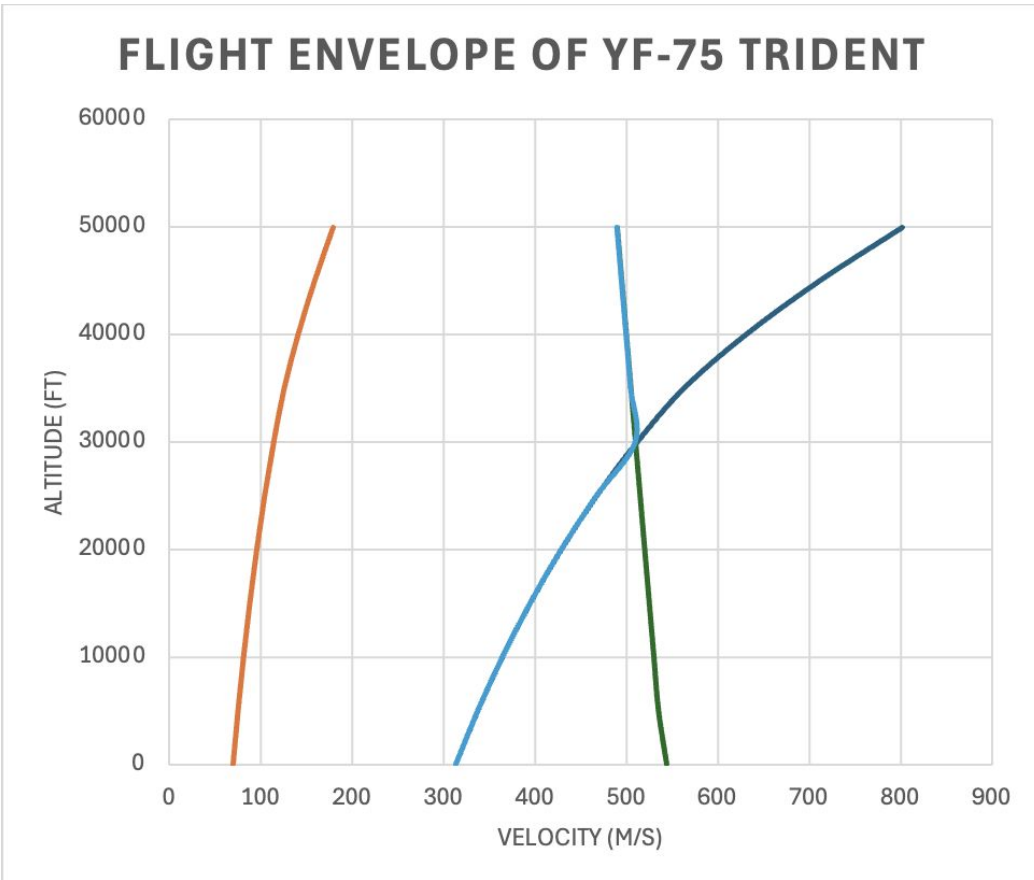

Figure 59: YFQ-75 Flight Envelope

The Flight Envelope for the YFQ-75, has been developed to indicate the operational limits of the aircraft across differing altitudes. The orange boundary line depicts the TRIDENT's stall limits, which increases as altitude increases due to decreasing air density. The upper boundary, depicts the aircrafts dynamic pressure and mach limit. As the altitude increase, the governing principle of the aircraft changes from dynamic pressure to mach limitations. This flight envelope demonstrates that the YFQ-75 TRIDENT can operate safely throughout the mission.

C. Takeoff and Landing distance metrics

The YFQ-75 TRIDENT will takeoff and land from the Navy's CVN 68/78 variant carriers during its operational life cycle. The RFP requires the aircraft to be able to take off from the carrier when the ambient conditions are 89.8°F with 0 wind over deck (WOD). The takeoff speed has been determined by utilizing Raymer's [1] stall equation (V_{Stall}). The speed required for takeoff is 1.2 times this value. The TRIDENT's takeoff speed for the Ground Strike mission profile has been evaluated to be 165 knots**.** Since the ground strike mission is the heavier configuration the TRIDENT will be able to take of in the Air to Air and Air to ground configurations. The CVN 68-78 can launch aircraft at about 150-170 knots, allowing the TRIDENT to successfully lift off the carrier.

$$Vstall=\sqrt{\frac{2w}{\rho S C_{lmax}}}$$

Where :
W= 48,750 lbs
ρ = 1.225 kg/m^3
S= 36.23m^2
Cl_{max}= 1.35

To validate the aircraft's ability to land, the same methodology has been utilized with the only deviation being a 1.3 multiplier to the stall speed. The TRIDENT's landing speed has been calculated to be 126 knots. This speed is acceptable for carrier operations and prove the TRIDENT's ability to land safely after missions.

$$Vstall=\sqrt{\frac{2w}{\rho S C_{lmax}}}$$

Where:
W= 33,814 lbs
ρ = 1.225 kg/m^3
S= 36.23m^2
Cl_{max}= 2.31

D. Dash Speed

To comply with RFP requirements, the TRIDENT has been designed to operate at high speeds across multiple altitudes allowing for rapid ingress and egress. The RFP requires the aircraft to operate at mach 1.6 at 30,000 feet and mach 0.9 at sea level. To ensure compliance to the RFP, the TRIDENT'S performance was evaluated using the following Raymer's [1] Dash speed equation.

$$\text{Dash Speed} = \sqrt{\frac{2(T)}{(\rho)(S)(C_{Do})}}$$

Where:
T= 32,500 lbf
ρ = 0.0008 slugs/ft^3 (At 30,000 ft)
S= 390 ft^2
$\mathbf{C_{Do}}$= 0.04006

The TRIDENT is required to have a dash speed of Mach 1.6 or 1,227 miles per hour, at an altitude of 30,000 feet above sea level. Calculation of the performance indicates the TRIDENTS is capable of reaching a dash speed of 2,280 ft/s equivalent to 1,554 miles per hour **.** Based on this result, the TRIDENT is in compliance with the RFP requirement.

In addition to the required dash speed at 30,00 feet, the TRIDENT is required to have a dash speed of 0.9 at sea level. To evaluate this performance metric, the same equation was utilized, however the air density value was manipulated to match the air density at sea level.

$$\text{Dash Speed} = \sqrt{\frac{2(T)}{(\rho)(S)(C_{Do})}}$$

Where:
T= 32,500 lbf
ρ = 0.0024 slugs/ft^3(at sea level)
S= 390 ft^2
$\mathbf{C_{Do}}$= 0.04006

Using this equation, the TRIDENT was calculated to achieve a dash speed of 1,316 ft/s equivalent to 897 miles per hour. This performance is higher than the required Mach 0.9 stipulated by the RFP, demonstrating the TRIDENTS compliance with the RFP requirement.

E. Range

The YFQ-75, has been designed to achieve a combat radius of 800 nautical miles during both mission sets, allowing it to be versatile while adhering to the RFP requirements. To evaluate the TRIDENT's range capability, the Breguet Range Equation was utilized. The mission was divided in sections, including cruise, combat , dash, and loiter. The fuel fraction for each of the segments were also individually evaluated.

$$\text{Breguet Range Equation:} R = \frac{V}{c}\frac{L}{D}\ln\left(\frac{W_i}{W_f}\right)$$

Where:
V= Velocity
c= Specific Fuel Consumption
L/D= Lift/ Drag Ratio
W_i= Weight Initial
W_f= Weight final

Where:

$$\text{Fuel Fraction:} e^{-\frac{Rc}{v(\frac{L}{D})}}$$

R= Range
c= Specific Fuel Consumption
v=Velocity
L/D= Lift/ Drag Ratio

Air To Ground:
The Air to Ground is the designed mission of the YF-75Q, the mission has been divided into 4 segments, namely cruise (inbound and outbound), dash, and loiter. Fuel fraction for each segment was also verified using the above mentioned endurance relation equation. To find combat radius, the total range was divided in half .Utilizing the Breguet equation, the aircraft has been evaluated to have a range of 838 nautical miles. This exceeds the designed goals of the TRIDENT, and adheres to the constraints of the RFP.

Mission Segment	Specific Fuel Consumption	Segment Weight (i) lbs	Segment Weight (f)	Fuel Fraction	Segment Range
Cruise (out)	0.75	48,750.0	43,875.0	0.90	717
Dash	0.75	43,875.0	42,997.5	0.98	61
Cruise (In)	0.75	42,997.5	38,697.7	0.90	716
Loiter	0.75	38,697.7	37,923.8	0.99	183
				TOTAL:	**838 nm**

Figure 60: Segment Range for Air to Ground Mission

Air To Air:
The Air to Air mission is the secondary mission of the YFQ-75, the mission has been divided into five segments, namely cruise (inbound and outbound), dash, combat, and loiter. Fuel fraction for each segment was also verified using the endurance equation discussed in the previous page. To find combat radius, the total range was divided in half Utilizing the Breguet equation, the aircraft has been evaluated to have a range of 857 nautical miles. This exceeds the designed goals of the TRIDENT, and adheres to the constraints of the RFP.

Mission Segment	Specific Fuel Consumption	Segment Weight (i) lbs	Segment Weight (f)	Fuel Fraction	Segment Range
Cruise (out)	0.75	35,848.0	32,263.2	0.90	717
Dash	2.10	32,263.0	31,617.9	0.98	45
Combat	2.10	31,617.9	30,985.5	0.98	51
Cruise (out)	0.75	30,985.5	27,887.0	0.90	717
Loiter	0.75	27,887.0	27,608.10	0.99	183
				TOTAL:	857 nm

Figure 61: Segment Range for Air to Air Mission

F. Sustained Turn Rate

The TRIDENT has been designed to achieve high sustained turn rates, which allow the aircraft to remain maneuverable and efficient during air to air engagement. The RFP requires the aircraft to be capable of achieving a sustained turn rate of 8-10 deg/s. To evaluate the TRIDENT's sustained turn rate, Raymer's [1] sustained turn rate equation was utilized. Utilizing this equation, the TRIDENT is calculated to achieve a sustained turn rate of 10.2 degrees, exceeding the desired turn rate and exceeding RFP requirements.

$$\text{Sustained Turn Rate: } \omega = \frac{g\sqrt{n^2-1}}{V}$$

Where:
g= 9.81 m/s
n= 1.3
V=102 m/s

Load factor was evaluated used a calculated load factor rather than a simulated load factor. The equation utilized, is as follows:

$$n = \frac{qC_l}{\frac{W}{S}}$$

Where:
q = 3396.06
$\mathbf{C_l}$= 1.8
W= 173,480 N
S= 36.23 m^2

XVIII. Mass Properties

A. Weight Buildup

I. Estimation Method

We are going to use a mix of the Raymer [1] computational method and the actual known component weights to calculate the weight of each component. If weights of component aren't available, then Raymer's method will be used. It can be noted that in the Raymer computations, it will occasionally combine different components into one section such as the weight of air conditioning and anti-ice are assumed to be in the same mass calculation and in one component mass. Whereas, calculating the weight of flight controls only contains the weight of the flight controls and no other components. This will be reflected in the following table where each component will be shown alongside its corresponding Raymer equations.

Component Mass Equations

Component	Raymer 7th Edition
Exposed Wing Structure	15.1
Horizontal Tail	15.2
Vertical Tail	15.3
Fuselage Structure	15.4
Main Landing Gear	15.5
Nose Landing Gear	15.6
Uninstalled Engine	Actual Weight Used
Air Induction System	15.10
Engine Cooling	15.12
Oil Cooling	15.13
Engine Controls	15.14
Starter	15.15
Fuel Systems/ Tanks	15.16
Flight Controls	15.17
Instruments	15.18
Hydraulics	15.19
Electrical	15.20
Avionics	15.21
Air Conditioning	15.23
Anti Ice	15.23

Figure 62: Raymer Equations for each major Empty Weight Component

II. Component Masses

In this section, a component by component weight comparison will be made between the YFQ-75 and the F/A-18E for both the strike (Design Mission) and air-to-air (Off-Design Mission) mission profiles. This comparison is appropriate as the RFP calls for a replacement aircraft that is capable of conducting similar missions that the F/A-18E/F currently does. By comparing component weights across identical mission profiles, any significant differences created by difference in engines, manned vs. unmanned, our composite skin, or one of the many other deviations from the F/A-18E can be identified and justified. This will ensure that our design, although significantly different in weight (shown in Figures 63-66) and general design, has a physically realistic weight breakdown consistent with other carrier-based multirole strike fighters of this class.

YFQ-75 Strike Profile

Component	Mass (lbs)
Empty Weight	**17734**
Wing	2895
Horizontal Tail	412
Vertical Tail	284
Fuselage Assembly	3319
Main Gear Assembly	966
Nose Gear Assembly	249
Engine	4050
Air Induction System	385
Engine Cooling	267
Oil Cooling	38
Engine Controls	17
Starter	67
Fuel Systems/ Tanks	678
Flight Controls	844
Instruments	0
Hydraulics	242
Electrical	893
Avionics	1858
Air Conditioning / Anti Ice	272
Useful Load Components	**29422**
Flight Crew	0
External Store Suspension and Release Equipment (Pylons and Launchers / Ejectors)	497
Gun	0
External Weapons	4428
External Fuel Tanks	762
Internal Fuel	16048
External Fuel 1 - Usable	3264
External Fuel 2 - Usable	3264
Fuel - Trapped	1159
MTOW	47156

Figure 63: YFQ-75 Strike Component Breakdown

F/A-18E Strike Profile

Component	Mass (lbs)
Empty Weight	**27983**
Wing	4321
Horizontal Tail	579
Vertical Tail	847
Fuselage Assembly	6844
Main Gear Assembly	946
Nose Gear Assembly	309
Engine	4890
Air Induction System	1583
Engine Cooling	239
Oil Cooling	38
Engine Controls	20
Starter	59
Fuel Systems/ Tanks	2961
Flight Controls	768
Instruments	195
Hydraulics	242
Electrical	924
Avionics	1858
Air Conditioning / Anti Ice	361
Useful Load Components	**30144**
Flight Crew	360
External Store Suspension and Release Equipment (Pylons and Launchers / Ejectors)	497
Gun	494
External Weapons	4376
External Fuel Tanks	1524
Internal Fuel	14700
External Fuel 1 - Usable	3264
External Fuel 2 - Usable	3264
Fuel - Trapped	1665
MTOW	58127

Figure 64: F/A-18E Strike Component Breakdown

YFQ-75 Air-to-Air Profile	
Component	**Mass (lbs)**
Empty Weight	**17734**
Wing	2895
Horizontal Tail	412
Vertical Tail	284
Fuselage Assembly	3319
Main Gear Assembly	966
Nose Gear Assembly	249
Engine	4050
Air Induction System	385
Engine Cooling	267
Oil Cooling	38
Engine Controls	17
Starter	67
Fuel Systems/ Tanks	678
Flight Controls	844
Instruments	0
Hydraulics	242
Electrical	893
Avionics	1858
Air Conditioning / Anti Ice	272
Useful Load Components	**16401**
Flight Crew	0
External Store Suspension and Release Equipment (Pylons and Launchers / Ejectors)	431
Gun	0
External Weapons	2512
External Fuel Tanks	0
Internal Fuel	12696
External Fuel 1 - Usable	0
External Fuel 2 - Usable	0
Fuel - Trapped	762
MTOW	34135

Figure 65: YFQ-75 Air-to-Air Component Breakdown

F/A-18E Air-to-Air Profile	
Component	**Mass (lbs)**
Empty Weight	**27983**
Wing	4321
Horizontal Tail	579
Vertical Tail	847
Fuselage Assembly	6844
Main Gear Assembly	946
Nose Gear Assembly	309
Engine	4890
Air Induction System	1583
Engine Cooling	239
Oil Cooling	38
Engine Controls	20
Starter	59
Fuel Systems/ Tanks	2961
Flight Controls	768
Instruments	195
Hydraulics	242
Electrical	924
Avionics	1858
Air Conditioning / Anti Ice	361
Useful Load Components	**16597**
Flight Crew	360
External Store Suspension and Release Equipment (Pylons and Launchers / Ejectors)	385
Gun	494
External Weapons	1072
External Fuel Tanks	0
Internal Fuel	13477
External Fuel 1 - Usable	0
External Fuel 2 - Usable	0
Fuel - Trapped	809
MTOW	44580

Figure 66: F/A-18E Air-to-Air Component Breakdown

As shown above, the YFQ-75 being consistently significantly lighter than the F/A-18E/F on a component-by-component basis is a result of the use of composite materials throughout the airframe, smaller aircraft overall, and lack of manned utility, as opposed to the manned, larger, and mostly aluminum structure of the F/A-18E/F. Despite the structural weight savings, the proposed aircraft carries a greater fuel weight than the F/A-18E/F, reflecting the more demanding performance requirements outlined in the RFP, which are specifically the 700-1,000 nm combat radius, Mach 1.6 dash speed, and sustained turn rate requirements. With these structural weight savings, the aircraft is now capable of carrying the additional fuel necessary to meet these performance targets while remaining within the RFP's 90,000 lb maximum takeoff gross weight constraint.

B. Center of Gravity

The aerodynamic center of the proposed aircraft is calculated to be located approximately 23.65 ft aft of the nose, which is derived from the horizontal tail moment arm of 19.35 ft and the overall aircraft length of 43 ft. At takeoff with full fuel and strike ordnance loaded, the center of gravity is located slightly aft of the aerodynamic center, at approximately 25 ft from the nose. This places the aircraft in a mildly statically unstable state in the longitudinal axis, with an estimated static margin of approximately -5% to -10%.

This mild static instability is consistent with modern high-performance fighter design philosophy, as shown by the F-16, F-22, and F-35, all of which operate with negative static margins to enhance agility and maneuverability. A statically unstable aircraft is inherently more responsive to control inputs, which directly benefits the sustained turn rate and dash speed requirements outlined in the RFP. For a conventionally manned aircraft this would necessitate a fly-by-wire flight control system to maintain safe and controllable flight. However, for the TRIDENT, the flight control computer will manage this instability, making the configuration not only acceptable but advantageous for the demanding combat maneuvering requirements of the mission at hand.

As fuel is burned throughout the mission, the center of gravity will shift aft due to the forward positioning of the fuel tanks relative to the aerodynamic center. However, given the unmanned and autonomous nature of the TRIDENT, this shift is continuously managed by the flight control computer in real time, which actively adjusts control surface deflections to compensate for any changes in static margin throughout the flight envelope. This level of autonomous stability management is standard in modern fly-by-wire systems and ensures the aircraft remains controllable and within acceptable stability limits across all mission segments without the limitations imposed by a human pilot's tolerance for instability.

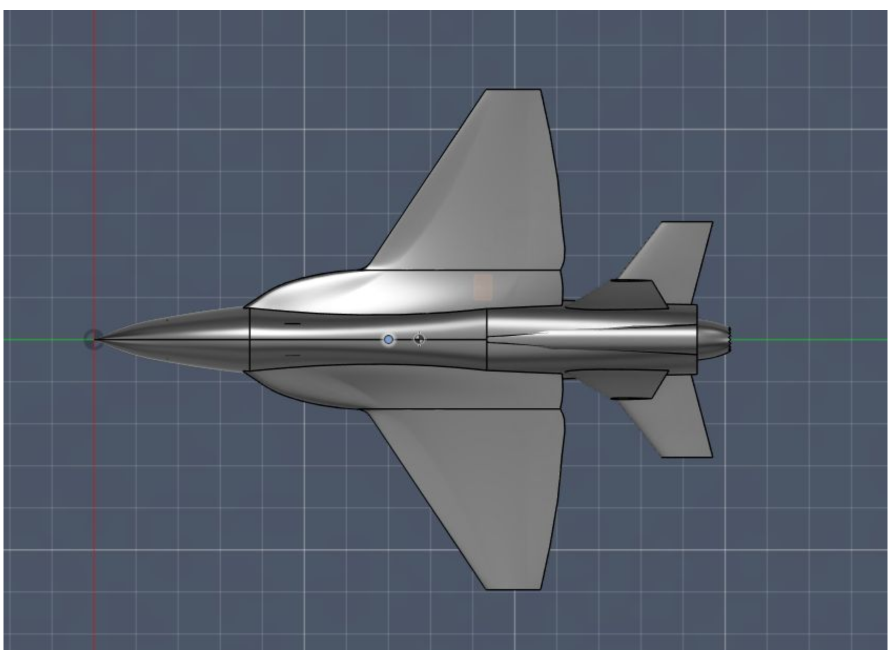

Figure 67: Center of Gravity (Checkered) vs. Aerodynamic Center (Blue)

XIX. Maintenance & Carrier Operations

A. Maintenance Philosophy

The maintenance philosophy for the YFQ-75 Trident was developed in alignment with the design decisions established by the Preliminary Design Review (PDR), where internal component placement and access panel locations were selected to minimize maintenance complexity and support high turnaround rates. The primary philosophy adopted is Single Layer Direct Access, ensuring that all internal components are reachable without requiring the removal of other components in the process. This is achieved through deliberate placement of internal components and strategic distribution of maintenance panels throughout the airframe. As Raymer notes, accessibility is fundamentally dependent on packaging density, door placement, and the number of components that must be displaced to reach a broken part [1]. To minimize downtime and simplify troubleshooting, certain components have been grouped in close proximity, reducing the number of access points a technician must check to isolate a problem.

Maintenance panel placement follows the principle that the best access should be provided to the components that fail most frequently or demand the most routine servicing [1]. In accordance with this, large access doors have been incorporated for the engine, avionics compartment, hydraulic pumps, actuators, electrical generators, and auxiliary power unit, ensuring that the most maintenance-intensive systems remain readily exposed without extensive disassembly [1]. This design approach directly supports the three-level NAMP maintenance framework, enabling O-level technicians to perform routine servicing quickly at the flight line while reserving more complex access for I-level and D-level activities. This SLDA architecture is a direct contributor to the YFQ-75 Trident's estimated MMH/FH of 7.6, as the reduction in access time and collateral maintenance significantly lowers the total labor hours required per flight hour.

B. Maintenance Routine

Repair and Maintenance for the YFQ-75 Trident involves the implementation of a maintenance schedule as shown in figure 68, ensuring operational readiness and airworthiness throughout the aircraft's service life. Following the Naval Aviation Maintenance Program (NAMP), maintenance is classified into three levels based on technical complexity, depth, and scope of work: Organizational (O-level), Intermediate (I-level), and Depot (D-level). O-level maintenance is the most routine, performed directly by the operating unit on its assigned aircraft, and includes inspection, servicing, lubrication, adjustment, and replacement of minor parts and subassemblies, prioritizing quick turnaround to maximize operational availability. I-level maintenance is performed by designated Intermediate Maintenance Activities (IMA) and focuses on producing ready-for-issue parts and ready-for-use support equipment, encompassing component inspection, testing, repair, calibration, and Non-Destructive Inspection (NDI) of airframe and dynamic components when required. D-level maintenance represents the most extensive rework, performed at depot facilities managed by COMNAVAIRSYSCOM or original equipment manufacturer sites, and includes aircraft overhaul, engine rework, modification, manufacture of parts, and technical engineering assistance beyond the capability of O and I-level activities [45].

The implementation of this three-level maintenance framework ensures the YFQ-75 Trident remains operationally ready and airworthy throughout its service life, minimizing downtime while maintaining the reliability required for successful mission execution.

To ensure consistency across all servicing activities, maintenance documentation for the YFQ-75 Trident shall adhere to MIL-STD-3001 and MIL-HDBK-3001 for the preparation and formatting of U.S. Navy work package technical manuals [49, 50]. Furthermore, the aircraft shall meet the airworthiness certification criteria established in MIL-HDBK-516C, executed in accordance with NAVAIRINST 13034.1 flight clearance policies [51, 53]. This ensures technicians are provided with standardized work packages and procedures for all scheduled and unscheduled maintenance actions, including step-by-step component removal and reinstallation instructions at each applicable maintenance level.

Figure 68: YFQ-75 Trident Three-Level Maintenance Framework Summary [45]

Maintenance Level	Performed By	Location	Scope of Work	Complexity
O-Level (Organizational)	Operating Unit	Flight Line/Gate	Inspection, servicing, lubrication, minor part replacement	Low
I-Level (Intermediate)	Designated IMA	Intermediate Maintenance Facility	Component Repair, NDI, calibration, technical directives	Medium
D-Level (Depot)	COMNAVAIRSYSCOM / OEM	Depot Facility / OEM Site	Full overhaul, engine rework, modification, manufacturing	Very High

C. Maintenance Man Hours Per Flight Hour (MMH/FH)

The MMH/FH of the YFQ-75 Trident is estimated at approximately 7.6 MMH/FH. This was determined by using the legacy F/A-18 C/D Hornet baseline of 16.0 MMH/FH as a starting reference and systematically reducing that value to reflect the architectural differences of the Trident [48]. According to the Aircraft Maintenance Experience Design Handbook, maintenance labor is not evenly distributed across aircraft systems, with operational support tasks such as fueling, towing, and preflight inspections accounting for approximately 27 percent of total MMH/FH, while propulsion systems account for roughly 16 percent, and radar and avionics contribute approximately 18 percent of the total burden [46]. The YFQ-75 Trident eliminates three systems that collectively represent a significant portion of the F/A-18's maintenance burden: the Environmental Control System, which accounts for approximately 5.5 percent of total MMH/FH due to mandatory pressurization testing and bleed-air duct inspections [46]; the ejection seat and egress system, which contributes approximately 3.5 percent through calendar-based explosive cartridge replacements and specialized safety inspections [46]; and the forward gun bay, which accounts for approximately 2.0 percent through scheduled armament inspections and post-firing corrosion cleaning protocols [46]. Additionally, the Trident's single Pratt & Whitney F100 engine, compared to the twin-engine configuration of the F/A-18, reduces the propulsion maintenance contribution by half relative to the baseline. Finally, the application of Single Layer Direct Access across all major component bays introduces a maintainability multiplier derived from Chiesa's Design to Maintain Coefficient, reducing the physical hardware labor hours of the remaining systems by approximately 46.7 percent by ensuring every Line Replaceable Unit is directly accessible behind a single exterior panel without requiring removal of adjacent components [47].

D. Maintenance Hatches

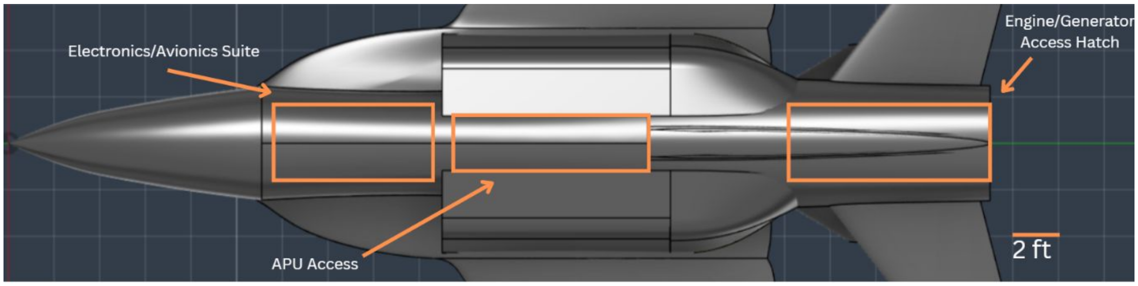

Figure 69: YFQ-75 Trident Bottom View - Maintenance Hatches

Three hinged access panels are located along the bottom fuselage of the YFQ-75 Trident. The forward panel sits directly behind and under the radar compartment and opens to expose the full electronics and avionics suite, which can be accessed from below through the nose landing gear wheel well when the landing gear is in the down position, providing ground-level access for O-level maintenance without the need for elevated platforms or additional equipment. The center panel accesses the Auxiliary Power Unit, positioned at the mid-rear fuselage, and is sized to permit full APU removal and replacement when required. The aft panel consolidates access to both the engine and the electrical generators behind a single hinged door, following Raymer's guidance that large access doors should be provided for engine systems and electrical generators to minimize disassembly time [1].

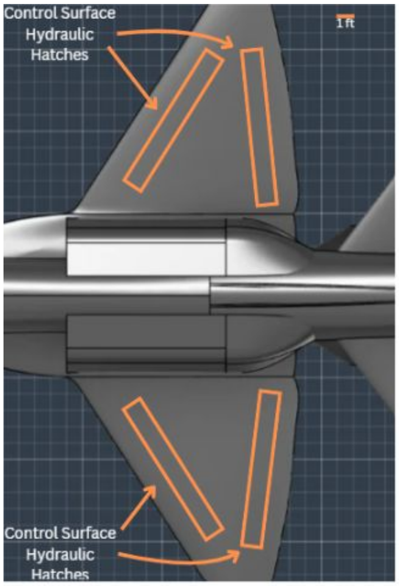

Figure 70: YFQ-75 Trident Bottom View - Control Surface Hydraulic Hatches

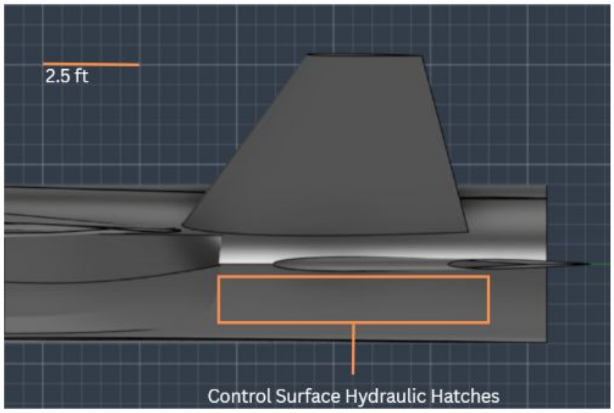

Figure 71: YFQ-75 Trident Side View - Control Surface Hydraulic Hatches

The control surface hydraulic hatches are hinged panels distributed across both the upper and lower wing surfaces at the elevon and leading edge slat regions. Each panel provides direct access to the aileron, elevator, and slat actuators without requiring removal of adjacent structural components. The rudder and stabilizer hydraulic lines share a common access panel at their structural intersection, consolidating two systems behind one opening and reducing total maintenance access points. This layout follows Raymer's principle that dedicated large doors should be provided for hydraulic pumps and actuators [1].

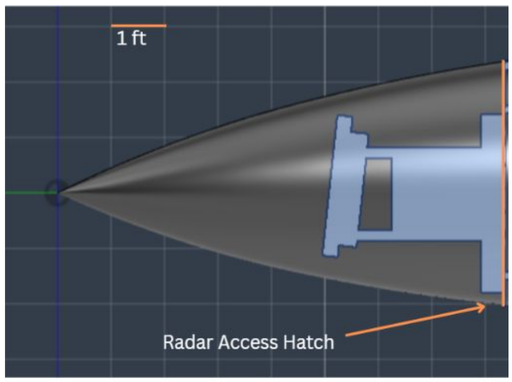

Figure 72: YFQ-75 Trident Side View - Radar Access Hatch

The radar access hatch is a swinging nose hatch positioned at the forward tip of the fuselage that opens to fully expose the radar antenna and waveguide assembly. Given that radar systems are among the most frequently maintained components on a naval aircraft, this hatch was deliberately designed to maximize exposure of the full antenna array in a single motion, eliminating the need to remove surrounding nose structure. This placement directly reflects Raymer's principle that the best access should be reserved for the components that break most often or require the most routine maintenance [1].

E. Carrier Compatibility

I. Takeoff

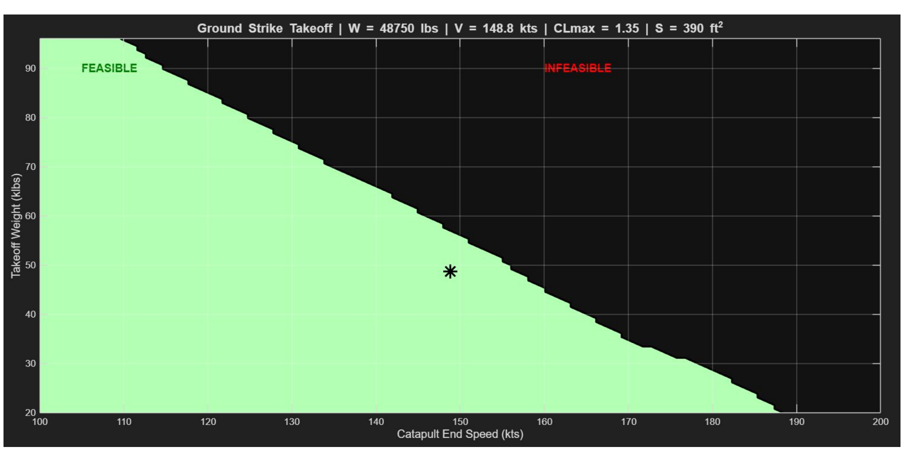

Figure 73: Takeoff Feasibility Analysis - Ground Strike Mission Profile

Carrier suitability for the YFQ-75 Trident was first evaluated under takeoff conditions using the C13-2 catapult performance curve provided in the RFP. The stall speed was computed from the lift equation:

$$V_{Stall} = \sqrt{\frac{2(W)}{(S)(\rho)(CL_{max})}}$$

where W = 48,750 lbs is the takeoff gross weight, S = 390 ft² is the wing area, ρ is the air density at sea level (0.002377 slug/ft³), and CL_{max} = 1.35. The minimum required catapult end speed was then determined as 1.15 times the stall speed, consistent with RFP Section 3.2.1. This required end speed was compared against the maximum end speed deliverable by the C13-2 catapult at each takeoff weight, interpolated directly from the RFP performance curve. The star marker denotes the YFQ-75 Trident's design point within the feasibility region, representing the aircraft's takeoff weight plotted against its required catapult end speed. The resulting design point of 148.8 knots falls within the feasible region, confirming the YFQ-75 Trident can be successfully launched from CVN-68 and CVN-78 class carriers under zero wind over deck conditions.

II. Landing

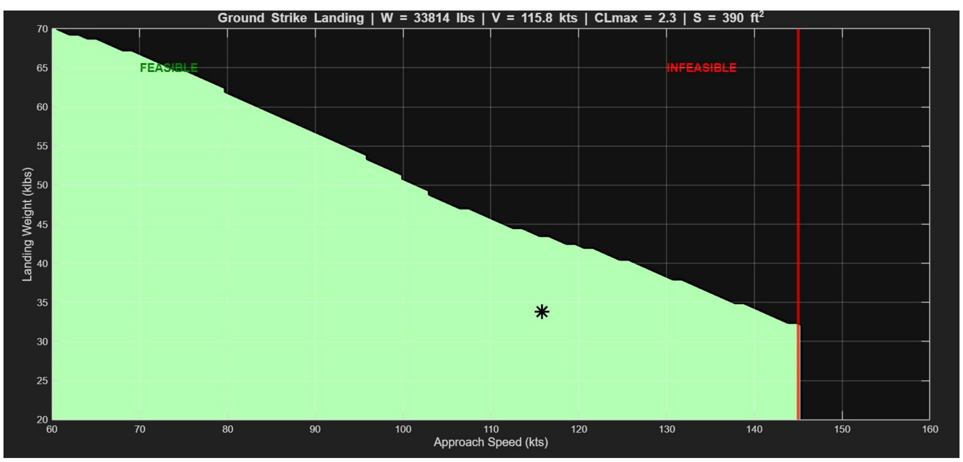

Figure 74: Landing Feasibility Analysis – Ground Strike Mission Profile

Recovery suitability was evaluated using the Mk7 Mod 3 arresting gear performance curve provided in the RFP. At a landing weight of 33,814 lbs, the stall speed was first computed using Equation 1 with a landing CL_{max} = 2.3 reflecting the higher lift coefficient achieved through deployment of flaps and slats in the landing configuration. The approach speed was then computed as 1.10 times the stall speed per RFP Section 3.2.2, with the arrestment engaging speed taken as 1.05 times the approach speed. Two constraints were enforced simultaneously: the approach speed must remain below 145 knots, and the landing weight must not exceed the arresting gear capacity at the computed engaging speed, interpolated from the RFP curve. The star marker denotes the YFQ-75 Trident's design point within the feasibility region, representing the aircraft's landing weight plotted against its approach speed. The resulting design point of 115.8 knots satisfies both conditions, confirming the YFQ-75 Trident meets all RFP recovery requirements.

III. Size

The YFQ-75 Trident was designed to meet all size and weight constraints specified in the RFP for carrier compatibility. The RFP requires an overall aircraft length not exceeding 50 feet, a folded wingspan not exceeding 35 feet, an overall aircraft height not exceeding 18.5 feet, and a maximum takeoff gross weight not exceeding 90,000 lbs per RFP Section 3.5. The YFQ-75 Trident satisfies all of these constraints with an overall length of 43 feet, a folded wingspan of 25.94 feet, an overall height of 12.35 feet, and a maximum takeoff gross weight of 48,750 lbs in its heaviest ground strike configuration, well within the 90,000 lb carrier elevator limit.

Figure 75: YFQ-75 Trident Geometric and Weight Constraint Compliance Summary

RFP Requirement	RFP Limit	YFQ-75 Trident
Overall Length	≤ 50 ft	43 ft
Folded Wingspan	≤ 35 ft	25.94 ft
Unfolded Wingspan	≤ 60 ft	35.68 ft
Overall Height	≤ 18.5 ft	12.35 ft
Max Takeoff Gross Weight (Ground Strike)	≤ 90,000 lbs	48,750 lbs
Min Takeoff Gross Weight (Air to Air)	≤ 90,000 lbs	35,848 lbs

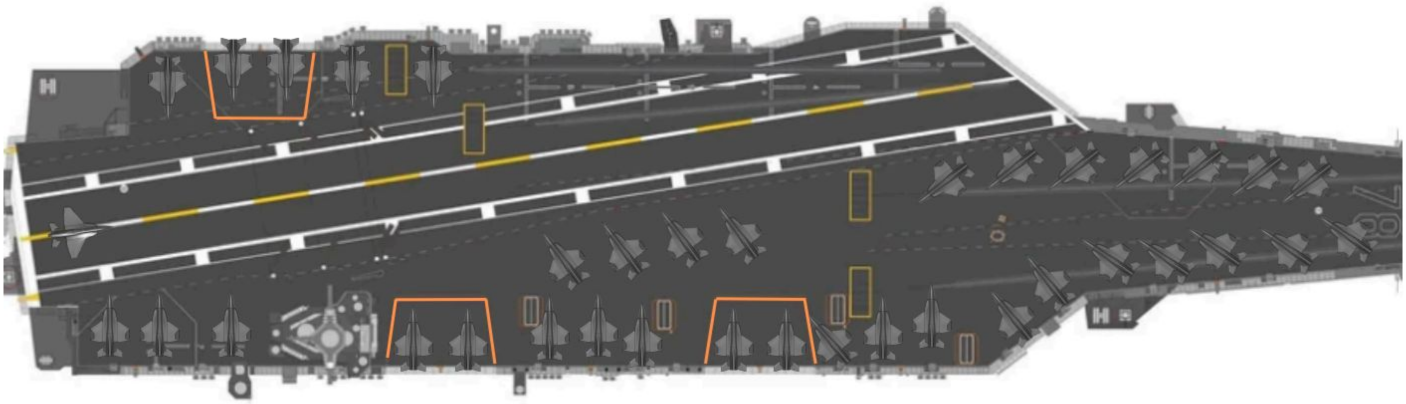

Figure 76: YFQ-75 Trident Deck Spotting and Elevator Clearance – CVN-78 Ford Class

Figure 76 illustrates the YFQ-75 Trident as deployed aboard a CVN-78 Ford-class carrier, satisfying the operational requirements for the two carrier classes specified in the RFP. The orange boxes denote the carrier elevator positions; the Trident's compact folded footprint of 25.94 feet confirms the aircraft fits within the elevator envelope, enabling seamless below-deck movement for storage and maintenance. This compact size maximizes deck spotting efficiency, supporting the high sortie-generation rates required for naval unmanned operations.

XX. Cost Analysis

Production Cases

In accordance with the Request for Proposal (RFP), this team has performed a cost analysis of a candidate strike fighter aircraft (YF-75) replacement for the FA-18E/F aircraft, while maintaining a comparable unit acquisition cost and enhancing performance. Here, we will provide the unit cost for a production run of 500 aircraft that maximizes cost-effective capability and minimizes development cost.

Lifecycle Cost Breakdown

The lifecycle cost of an aircraft refers to the total expenditure incurred during the design, production, operation, and disposal of the aircraft. Total lifecycle cost consists of the following categories: production (or flyaway cost), research, development, test, and evaluation (RDT&E), ground support equipment and initial spares (GSE&IS), special construction (SC), operation and maintenance (O&M), and disposal.

Flyaway Cost

Flyaway costs are the recurring costs of production to manufacture aircraft components such as the airframe, engine, and avionics [1]. This may also include tooling costs, manufacturer's overhead, and administrative expenses [1]. The flyaway cost per aircraft is reduced as more aircraft are produced due to the learning-curve effect [1]. (The learning-curve effect suggests that the more aircraft produced, the more the manufacturer learns, and the cheaper the next aircraft can be produced.) Production cost is generally up to half of the lifecycle cost for military aircraft [1].

Research, Development, Test, and Evaluation (RDT&E) Cost

RDT&E pertains to the fixed cost of aircraft conceptual design [1]. This category includes costs for technology research, design engineering, prototype fabrication, flight and ground testing, evaluations for operational suitability, and, for military aircraft, includes costs for demonstration of airworthiness, mission capability, and compliance with Military Specifications [1]. RDT&E is typically less than a tenth of the total life-cycle cost [1].

Operation and Maintenance (O&M) Cost

Operation and Maintenance (or Operation and Support) covers the cost for fuel, oil, ground personnel, maintenance, recurring costs, depot, insurance, various indirect costs, and depreciation, and is usually roughly equal to development and production costs in the military environment [1].

Ground Support Equipment and Initial Spares (GSE&IS) Cost

Military aircraft "procurement cost" (or "acquisition cost") refers to the costs of required ground support equipment & initial spares during operational deployment, such as flight simulators and test equipment [1].

Special Construction (SC) Cost

Special construction cost is the cost to build special or new ground facilities for the operational deployment of some aircraft that may require them [1]. Ultimately, special constructions contribute to the total program cost of developing and deploying a new aircraft into the military inventory [1].

Disposal

Disposal involves the cleaning, preservation, and storage of old aircraft at the end of their lifecycles [1]. This cost is small or negligible in early lifecycle cost estimations [1].

Lifecycle Cost Ratios

To maximize the accuracy of the unit acquisition cost estimation for the YF-75, all expenses in the above categories must be considered. Furthermore, as a rough breakdown for proportionality consistency, the approximate element contribution to lifecycle cost is summarized in Figure 77 and are as as follows: O&M contributes 55-65%, production contributes 30-40%, RDT&E contributes 5-10%, GSE&IS contributes 5-7%, special construction contributes 4-6%, and disposal contributes 0.05-1% toward lifecycle cost. Keeping these proportions during cost analysis is essential to ensure the team's aircraft total cost is not skewed disproportionately in any direction.

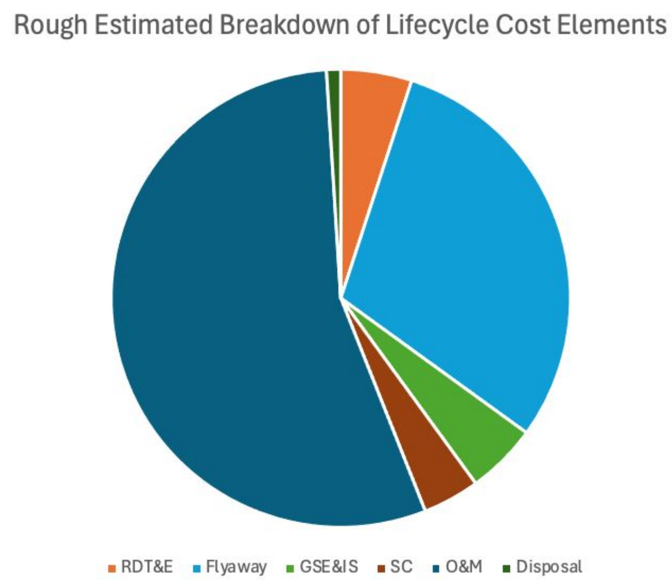

Figure 77: Lifecycle Cost Elements Ratios

<u>F/A-18E/F Super Hornet Unit Cost</u>

The Official U.S. Navy Website reports an approximate unit cost of $67.4 million, in fiscal year 2021 dollars, for one F/A-18E/F aircraft [2]. Adjusted to fiscal year 2025 dollars using Consumer Price Index (CPI) inflation estimations provided by the U.S. Bureau of Labor Statistics, the unit cost for an F/A-18E/F aircraft corresponds to approximately 80.16 million dollars per unit aircraft [3]. Assuming that this unit cost consists only of production cost, which is 30% to 40% of total lifecycle costs, the total lifecycle cost is estimated to range from approximately $200.4 million to $267.2 million per unit aircraft. This provides the YF-75 a baseline comparison for lifecycle cost.

<u>RDT&E and Flyaway Cost Computations</u>

The acquisition cost for the YF-75 was estimated using the RAND Corporation's Development and Procurement Costs of Aircraft (DAPCA IV) model as provided in Aircraft Design: A Conceptual Approach, Seventh Edition by Daniel P. Raymer [1]. This model is used to compute costs for engineering, tooling, manufacturing, quality control, development support, flight testing, manufacturing materials, and engine production, which are summed alongside avionics costs to compute total RDT&E and Flyaway Cost. The formulas used are given below:

Engineering hours $(H_E) = 5.18W_e^{0.777}V^{0.894}Q^{0.163}$

Tooling hours $(H_T) = 7.22W_e^{0.777}V^{0.696}Q^{0.263}$

Manufacturing hours $(H_M) = 10.5W_e^{0.82}V^{0.484}Q^{0.641}$

Quality Control hours $(H_Q) = 0.133H_M$

Devel support cost $(C_D) = 67.4W_e^{0.630}V^{1.3}$

Flight Test Cost $(C_F) = 1947W_e^{0.325}V^{0.822}FTA^{1.21}$

Manufacturing Materials Cost $(C_M) = 31.2W_e^{0.921}V^{0.621}Q^{0.799}$

Engine Production Cost $(C_{eng}) = 3112[9.66T_{max} + 243.25M_{max} + 1.74T_{turbine\ inlet} - 2228]$

$$RDT\&E + flyaway = H_ER_E + H_TR_T + H_MR_M + H_QR_Q + C_D + C_F + C_M + C_{eng}N_{eng} + C_{avionics},$$

where

W_e = empty weight

V = maximum velocity

Q = lesser production quantity or number to be produced in five years

FTA = number of flight-test aircraft

N_{eng} = total production quantity times number of engines per aircraft

T_{max} = engine maximum thrust

M_{max} = engine maximum Mach number

$T_{turbine\ inlet}$ = turbine inlet temperature

$C_{avionics}$ = avionics cost

The average wrap rates or direct salaries paid to employees in engineering, tooling, quality control, and manufacturing were derived from those provided in Raymer's book, as shown in Figure 78 below.

Category	Average Wrap Rate
Engineering (R_E)	\$115
Tooling (R_T)	\$118
Quality Control (R_Q)	\$108
Manufacturing (R_M)	\$98

Figure 78: Average Wrap Rates

Inputs for RAND DAPCA IV Model

The input parameters for the YF-75 were extracted from information about the F/A-18 engine, the assumed production quantity given for the F/A-18E/F's average annual production (in this case, 10 per year for 5 years or 50 aircraft, and 2 flight-test aircraft), and the estimated empty aircraft weight as shown in Figure 79. Further clarification regarding total avionics costs will be provided in the subsequent section.

Input Parameters	Abbreviation	Value
Empty Weight (kg)	W_e	12,700.586
Max velocity (km/hr)	V	1915.119 [2]
Lesser of production quantity or number to be produced in five years	Q	50 [4]
Number of flight-test aircraft (typically 2-6)	FTA	2
Total production quantity times number of engines per aircraft	N_eng	104
Engine maximum thrust (kN)	T_max	97.86 [5]
Engine maximum Mach number	M_max	1.8 [6]
Turbine inlet temperature (K)	T_turbine_inlet	1890 [7]
Avionics cost ($)	C_avionics	$667,324,992

Figure 79: Input Parameters for RAND DAPCA IV Calculations

Avionics Cost

The avionics cost consists of expenses for Electronic Warfare, Radar, Sensors, & Targeting, Mission Computers, and Communications, totalling a unit avionics cost of $12.8 million, or $667.3 million for 52 aircraft. Avionics cost is summarized in Figure 80.

Category	Description	Cost
Electronic Warfare	AN/ALQ-214 Integrated Defensive Electronic Countermeasures (IDECM) [8]	$3,808,536.37
Radar, Sensors, & Targeting	AN/APG-77 Radar [9]	$5,100,000.00
	AN/ASQ-228 Advanced Targeting Forward-Looking Infrared (ATFLIR) [10]	$3,000,000.00
Mission Computers	Distributed Targeting Processor - Networked (DTP-N) [11]	$624,636.55
Communications	MIDS-LVT(1) Ruggedized Mobile System [12]	$300,000.00
Unit Avionics Cost		**$12,833,172.92**
Total Avionics Cost (Qty: 52)		**$667,324,991.82**

Figure 80: Avionics Cost Breakdown

Additional RDT&E Expenses

Additional RDT&E expenses, not originally considered within the RAND DAPCA IV model, consist of weapons as required by the RFP, aircraft hardware, and development test systems, totalling a unit cost of $571.2 million. Additional RDT&E costs are summarized in Figure 81.

Category	Description	
Weapons	AIM-120C (6 per aircraft, 52 aircraft) [13]	$499,200,000.00
	AIM-9X (2 per aircraft, 52 aircraft) [14]	$49,088,000.00
	MK-83 JDAM (4 per aircraft, 52 aircraft) [15]	$6,922,240.00
Aircraft Hardware/Survivability	Engine Baffles (estimated)	$50,000.00
	Thermal Protection System (estimated)	$1,000,000.00
Development Test Systems	Modified X-62 VISTA [16] - Enhanced Maneuvering and Control Computer (EMC2) - Galleon Network Attached Storage (NAS)	$15,000,000.00
Total Additional Expenses		**$571,260,240.00**

Table 81: Additional RDT&E Expenses

Total RDT&E and Flyaway Cost

Utilizing these inputs, the RAND DAPCA model computed a total RDT&E + Flyaway Cost of $5.9 billion for 52 aircraft, or $115.1 million per unit aircraft, as summarized in Figure 82, with a breakdown by category percentage in Figure 83.

Category	Value
Engineering	$1,495,938,659.83
Tooling	$708,480,056.72
Manufacturing	$1,135,464,029.34
Quality Control	$166,426,584.87
Development Support	$479,648,796.96
Flight Testing	$48,452,912.43
Manufacturing Materials	$467,193,594.92
Engine Production	$790,923,732.68
Avionics Cost	$667,324,991.84
Additional Expenses	$571,260,240.00
Total RDT&E + Flyaway Cost (Qty: 52)	$6,531,113,599.60
Unit RDT&E + Flyaway Cost (Qty: 1)	**$125,598,338.45**

Figure 82: RDT&E and Flyaway Cost Computation

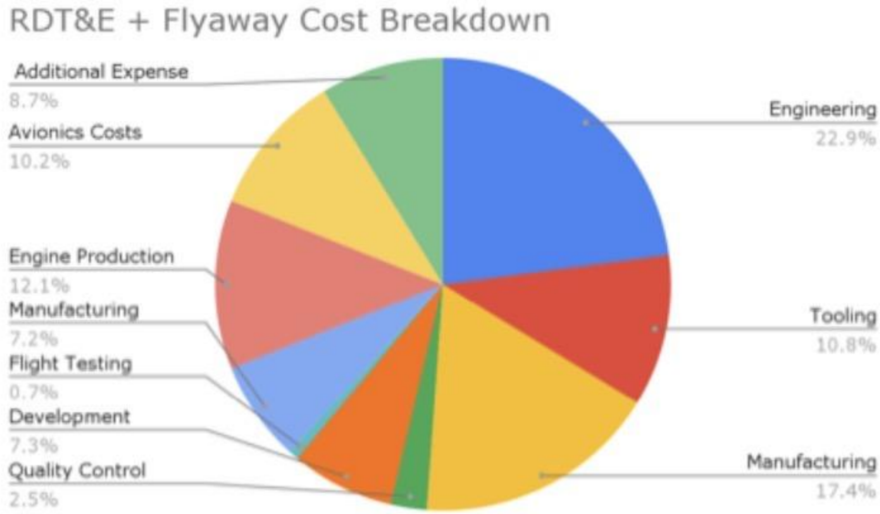

Figure 83: RDT&E + Flyaway Cost Total Breakdown by Category

Operation & Maintenance Costs

Operation and maintenance cost was estimated by determining the approximate operational cost per hour for maintenance, fuel consumption, training, logistics support, and other costs using that of the F/A-18E/F. This amount was then multiplied by estimated flight hours per year and subsequently multiplied by expected total operational years. The estimated operational cost per hour is $30,000 based on the F/A-18 E/F logistics [17]. The estimated flight hours per year is 200 [18]. Estimated total operational years are 30 years. Total operations & maintenance therefore total $180 million. Fuel, oil, aircrew personnel, ground personnel, insurance, maintenance, recurring costs, depot, indirect costs, depreciation of engine, and depreciation of airframe comprise the total O&M cost. Categorical percentage breakdown provided by Raymer's book was used to determine the appropriate allocation of the total O&M cost, as summarized in Figure 84.

Category	Percentage of Total O&M [1]	Cost
Fuel	14.5%	$26,100,000.00
Oil	0.50%	$900,000.00
Aircrew personnel	17.5%	$31,500,000.00

Ground personnel	17.5%	$31,500,000.00
Insurance	2%	$3,600,000.00
Maintenance, Recurring, Depot, Depreciation (engine), Depreciation (airframe), and various indirect costs	48%	$86,400,000.00

Figure 84: Operations and Maintenance Cost by Category

However, since the YF-75 is an unmanned aircraft, aircrew personnel training expenses are not needed and must be removed from the total. Removing the estimated aircrew personnel training cost of $31.5 million from the original total of $180 million brings the final O&M cost estimation to $148.5 million. Figure 85 showcases O&M costs by category. Maintenance constitute majority of total O&M, which is reasonable given the aircraft must be maintained recursively throughout its lifecycle.

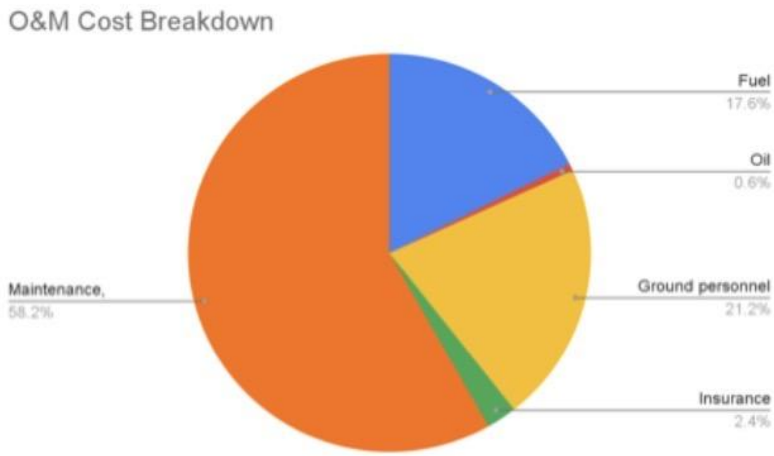

Figure 85: Operations and Maintenance Cost by Category (without aircrew training expenses)

Ground Support Equipment and Initial Spares

GSE&IS costs are derived from expenses made for the F/A-18 E/F aircraft, which include Munitions Handling and Loading Unit (MHU-83D/E Bomb Loader), Aerial Stores Lift Truck (MJ-1C Bomb Loaders), Universal Hydraulic Test Stand (UHTS), Tow Tractors, and Small Support Vehicles. Other expenses, such as Verification/Diagnostic Set and Portable Hydraulic Test Stands/Rigs/Power Supply, were estimated. The cost for a fully carbon fiber composite airframe was also implemented, bringing the total unit GSE&IS cost to $22.7 million as summarized in Figure 86.

GSE&IS	Costs
Munitions Handling and Loading Unit (MHU-83D/E Bomb Loader) [19]	$91,000.00
Aerial Stores Lift Truck (MJ-1C Bomb Loaders) [20]	$8,048.00
Universal Hydraulic Test Stand (UHTS) [21]	$22,348,042.00
Tow Tractors, Small Support Vehicles [22]	$30,000.00
Verification/Diagnostic Set - Flow, Pressure, Temperature (estimated)	$100,000.00
Portable Hydraulic Test Stands/Rigs/Power Supply (estimated)	$100,000.00
Carbon Fiber Composite IM7 (for wing and aircraft surface area) [23]	$73180.75
Unit GSE&IS Cost	**$22,750,270.75**

Figure 86: Ground Support Equipment and Initial Spares Cost

Special Construction and Disposal

Cost information about many special construction expenses is not publicly available. Thus, costs for this category were estimated to reflect typical lifecycle cost proportions; special construction should comprise 4-6% toward total lifecycle cost. The special construction costs are summarized in Figure 87.

Special Construction	
MF-500 Urethane RF Absorbing Coating Facility (estimated)	$1,000,000.00
Fabric Hangars Help FRCSW Preservation Program [24]	$2,500,000.00
Depot Maintenance/Minor Building Upgrades (estimated)	$1,500,000.00
Electrical/HVAC for Hangers (estimated)	$500,000.00
Security (estimated)	$150,000.00
Miscellaneous enhancements (estimated)	$500,000.00
Unit Special Constructions Cost	**$6,150,000.00**

Figure 87: Special Construction Costs

Similarly, cost information about disposal expenses is not publicly available. Thus, costs for this category were estimated to reflect typical lifecycle cost proportions; disposal should comprise 0.05-1% toward total lifecycle cost. The unit disposal costs are summarized in Figure 90.

Disposal	
Pickling	$500,000.00
Storage	$500,000.00

Other	$500,000.00
Unit Disposal Cost	**$1,500,000.00**

Figure 90: Disposal Costs

Overall Lifecycle Cost

By aggregating the unit costs for each lifecycle cost category as found above for RDT&E, Flyaway, O&M, GSE&IS, Special Construction, and Disposal, the total unit cost for the YF-75 can be found to be approximately $304.4 million. For a production run of 500 aircraft, this totals to $152.2 billion.

Lifecycle Cost Category	Unit Cost	Production Run for 500 Aircraft	Percentage of LCC
RDT&E + Production	$125,598,338.45	$62,799,169,225.00	41.26%
O&M	$148,500,000.00	$74,250,000,000.00	48.78%
GSE&IS	$22,693,045.47	$11,346,522,733.00	7.45%
SC	$6,150,000.00	$3,075,000,000.00	2.02%
Disposal	$1,500,000.00	$750,000,000.00	0.49%
Total Lifecycle Cost	**$304,441,383.92**	**$152,220,691,958.00**	**100.00%**

Figure 91: Total Lifecycle Cost for the YF-75

Final Assessment

Augustine's Law predicts that the unit cost of military aircraft rises exponentially over time [25]. The predicted acquisition cost for a military aircraft in the introduction year of 2030 is over or around $1 billion [25]. In comparison, the YF-75's estimated unit lifecycle cost is $304.4 million as detailed in Figure 91. Since flyaway (or acquisition) cost is approximately 30% of lifecycle cost, the acquisition cost for one YF-75 is approximately $91.5 million. Assuming an introduction year of 2030, this falls below the projected trend line predicted by Augustine's Law, successfully breaking the exponential cost trend.

XXI. References

[1] Raymer, Daniel. Aircraft Design: A Conceptual Approach, Seventh Edition. 15 Aug. 2024.

[2] U.S. Navy. "F/A-18E/F Super Hornet | NAVAIR." Navy.mil, 2020, www.navair.navy.mil/product/FA-18EF-Super-Hornet.

[3] U.S. Bureau of Labor Statistics. "CPI Inflation Calculator." U.S. Bureau of Labor Statistics, 2025, www.bls.gov/data/inflation_calculator.htm.

[4] National Naval Aviation Museum. "F/A-18 Hornet (Tactical)." Public2.Nhhcaws.local, www.history.navy.mil/content/history/museums/nnam/explore/collections/aircraft/f/f-a-18-hornet--tactical-.html.

[5] Spray, Aaron. "How Many F-35, F-15 & F/A-18 Fighter Jets Did the US Industry Deliver in 2024?" Simple Flying, 28 Jan. 2025, simpleflying.com/how-many-f-35-f-15-f-a-18-fighter-jets-us-industry-delivered-2024/.

[6] GE Aerospace. "F414 Engine | GE Aerospace." Www.geaerospace.com, www.geaerospace.com/military-defense/engines/f414.

[7] Tugraz. "Historical-Trends-of-of-Fighter-Engine-Problems." Tugraz.at, 2026, aeroenginesafety.tugraz.at/lib/exe/fetch.php?media=:11:111:historical-trends-of-of-fighter-engine-problems.svg. Accessed 10 Mar. 2026.

[8] U.S. Department of War. "Contracts for Mar. 3, 2021." U.S. Department of War, 2021, www.war.gov/News/Contracts/Contract/Article/2523684/contracts-for-mar-3-2021/.

[9] Forecast International. "EAN130A1_APG-77 v Archived OCT." Forecast International, Oct. 2012, www.forecastinternational.com/archive/disp_pdf.cfm?DACH_RECNO=942.

[10] Deagle. "AN/ASQ-228 ATFLIR." Guide to Military Equipment and Civil Aviation, 2016, www.deagel.com/Components/ANASQ-228%20ATFLIR/a001647.

[11] U.S. Department of War. “Contracts for Jun. 3, 2021.” U.S. Department of War, 2021, www.war.gov/News/Contracts/Contract/Article/2644648/contracts-for-jun-3-2021/.

[12] Forecast International. “EES130A1_USQ-140 Multifunctional Information.” Forecast International, Sept. 2006, https://www.forecastinternational.com/archive/disp_pdf.cfm?DACH_RECNO=631#:~:text=Price%20Range.,each)%20for%20the%20United%20States.

[13] Mahir Zeynalov. “The Silent Hunter: Ultimate Guide to the AMRAAM Missile.” The Defense Post, July 2025, thedefensepost.com/2025/07/01/amraam-missile-guide/.

[14] Hollings, Alex. “You’re Probably Thinking of Missile Costs All Wrong.” Sandboxx, 7 Nov. 2023, www.sandboxx.us/news/youre-probably-thinking-of-missile-costs-all-wrong/.

[15] Official United States Air Force Website. “Joint Direct Attack Munition GBU- 31/32/38.” U.S. Air Force, www.af.mil/About-Us/Fact-Sheets/Display/Article/104572/joint-direct-attack-munition-gbu-313238/.

[16] Foose, Patrick. “Modified X-62 Helps Accelerate Tactical Autonomy Development.” ONE AFRL / TWO SERVICES, 19 Aug. 2022, www.afrl.af.mil/News/Article-Display/Article/3133468/modified-x-62-helps-accelerate-tactical-autonomy-development/.

[17] Oreate AI Blog. “The Cost of F/A-18 Super Hornet: A Look at Its Value and Capabilities.” Oreate.com, 19 Jan. 2026, www.oreateai.com/blog/the-cost-of-fa18-super-hornet-a-look-at-its-value-and-capabilities/467a814dddfdb297ef1bfdbbb055267f.

[18] Naval Air Systems Command. “F/A-18 and EA-18G Surpass 12 Million Flight Hours | NAVAIR.” Navy.mil, 2025, www.navair.navy.mil/news/FA-18-and-EA-18G-surpass-12-million-flight-hours/Fri-08012025-1008.

[19] Air Force Material Command. “Ogden ALC Saves Time, Money with MHU-83 Lift Work.” Air Force Materiel Command, 7 Aug. 2015, www.afmc.af.mil/News/Article-Display/Article/803857/ogden-alc-saves-time-money-with-mhu-83-lift-work.

[20] Comptroller General of the United States. “Comptroller General of the United States.” *United States General Accounting Office*, 3 Mar. 1972, www.gao.gov/assets/b-173788.pdf#:~:text=Originally%20this%20contract%20was%20for%2081%20MJ%2D1,official%20designation%20of%20the%20trucks%20to%20A/S32K%2D3.

[21] Hydraulics International (Asia). “Air Force Hydraulic Test Equipment.” *Hydraulics International (Asia)*, 31 Dec. 2016, hiigroupasia.com/air-force-hydraulic-test-equipment/.

[22] Legacy GSE. “Aircraft Tow Tractors & Baggage Tugs.” *Legacy GSE- Used Ground Support Equipment*, 2020, www.legacygse.com/tow-tractors--tugs.html.

[23] Composite Envisions. “Carbon Fiber Fabric Plain Weave Intermediate Modulus 6k 6.13oz/208gsm Hexcel IM7.” *Compositeenvisions.com*, 2026, www.compositeenvisions.com/Carbon-Fiber-Fabric-Plain-Weave-6k-6.13oz-208gsm-Hexcel-IM7?quantity=1&width=624.

[24] U.S. Department of War . “Fabric Hangars Help FRCSW Preservation Program | NAVAIR.” *Navy.mil*, 2016, www.navair.navy.mil/node/24381.

[25] Allen, Gregory C, and Isaac Goldston. “Updating Augustine’s Law: Fighter Aircraft Cost Growth in the Age of AI and Autonomy.” Csis.org, 2024, www.csis.org/analysis/updating-augustines-law-fighter-aircraft-cost-growth-age-ai-and-autonomy.

[26] “AN/APG-79 AESA Radar.” @RaytheonTech, 2025, www.rtx.com/raytheon/what-we-do/air/apg79aesa.

[27] APG-63(V). Forecast International , Apr. 2021, pp. 1–12.

[28] APG-77(V). Forecast International , Oct. 2012, pp. 1–7.

[29] ASQ-228/Advanced Targeting Forward-Looking Infared (ATFLIR). Forecast International , Nov. 2023, pp. 1–13.

[30] “Boeing F/A-18 Nose Landing Gear.” Safran, 2020, www.safran-group.com/products-services/boeing-fa-18-nose-landing-gear.

[31] Cotting, Christopher, et al. "X-62 VISTA Capabilities and Architecture | AIAA SciTech Forum." AIAA SciTech Forum, 2023, https://doi.org/10.2514/MSCITECH23;article:article:10.2514/6.2023-1744;groupTopic:topic:long_toc_pubs. Accessed 13 May 2026.

[32] "Distributed Targeting Processor - Networked (DTP-N)." L3Harris® Fast. Forward., 2020, www.l3harris.com/all-capabilities/distributed-targeting-processor-networked-dtp-n.

[33] "MIDS-LVT Terminals." L3Harris® Fast. Forward., 2020, www.l3harris.com/all-capabilities/mids-lvt-terminals. Accessed 13 May 2026.

[34] Rudowsky, Thomas, et al. UNCJL/^SfFIED TECHNICAL REPORT REVIEW of the CARRIER APPROACH CRITERIA for CARRIER-BASED AIRCRAFT PHASE I; FINAL REPORT. 2002, apps.dtic.mil/sti/tr/pdf/ADA411068.pdf. Accessed 13 May 2026.

[35] Section 3 DATA SECTION-TIRES Three-Part Name Sizes. www.goodyearaviation.com/resources/pdf/tire-specifications-6-2018.pdf.

[36] SURVIVABILITY for MISSION SUCCESS. July 2019, www.l3harris.com/sites/default/files/2020-08/l3harris-an-alq-214-idecm-sell-sheet-sas.pdf.

[37] VALID. NATOPS FLIGHT MANUAL NAVY MODEL F/A-18E/F 165533 and up AIRCRAFT THIS PUBLICATION SUPERSEDES A1-F18EA-NFM-000 DATED 1 DECEMBER 2004 CHANGED 1 AUGUST 2006. 2009, info.publicintelligence.net/F18-EF-000.pdf.

[38] "VISTA." Lockheed Martin, 2024, www.lockheedmartin.com/en-us/products/x-62a-vista.html.

[39] "Weapons Carriage and Release Systems." L3Harris® Fast. Forward., 2020, www.l3harris.com/all-capabilities/weapons-carriage-and-release-systems. Accessed 13 May 2026.

[40] "X62A Vista." Www.edwards.af.mil, www.edwards.af.mil/Units/X62A-Vista/.

[41] Baesystems.com, 2024, www.baesystems.com/en/product/flight-control-systems.

[42] "NATOPS FLIGHT MANUAL NAVY MODEL F/A-18E/F 165533 and up AIRCRAFT (PERFORMANCE DATA)." 2001, info.publicintelligence.net/F18-EF-200.pdf. Accessed 13 May 2026.

[42] Selected Acquisition Report (SAR) F/A-18E/F. Dec. 2012, www.esd.whs.mil/Portals/54/Documents/FOID/Reading%20Room/Selected_Acquisition_Reports/FY_2012_SARS/F-A-18E-F_December_2012_SAR.pdf. Accessed 13 May 2026.

[43] Boeing F/A-18E/F & EA-18G Capabilities Brochure. Eaton, www.eaton.com/content/dam/eaton/markets/aerospace/Boeing-FA18EF-EA18G-capabilities-brochure.pdf. Accessed 13 May 2026.

[44] "F/A-18 Super Hornet and EA-18 Growler Technical Specifications." Boeing, www.boeing.com/defense/fighters-and-bombers/fa-18-super-hornet-and-ea-18-growler#technical-specifications. Accessed 13 May 2026

[45] THE NAVAL AVIATION MAINTENANCE PROGRAM (NAMP) Overview of the Naval Aviation Maintenance Program (NAMP) and Guide to the NAMP Instruction Chapter 2 Chief of Naval Operation and Commandant of the Marine Corps, System Commands, Aircraft Controlling, Navy Type Wings and Marine Air Wing, and Operational Commanders. 2021.

[46] Corporation, Vought. "Aircraft Maintenance Experience Design Handbook 0 - DTIC." AIRCRAFT MAINTENANCE EXPERIENCE DESIGN HANDBOOK, Sept. 1979, apps.dtic.mil/sti/tr/pdf/ADA090563.pdf.

[47] RAMS and Maintenance Cost Assessment in a Multidisciplinary Design Optimization Environment. 2019, elib.dlr.de/133800/1/Giovingo_Thesis_FINAL.pdf. Accessed 13 May 2026.

[48] Worldofaviation.com, 2026, worldofaviation.com/2019/01/super-squadron-super-hornet-training-at-nas-lemoore/. Accessed 13 May 2026.

[49] DEPARTMENT OF DEFENSE. PREPARATION of DIGITAL TECHNICAL INFORMATION for MULTI-OUTPUT PRESENTATION of TECHNICAL MANUALS (PART 1 of 8 PARTS). quicksearch.dla.mil/Transient/3CB32C48E1364C66952A9FD38DE35C19.pdf. Accessed 13 May 2026.

[50] "MIL-HDBK-3001 GUIDE to STYLE FORMAT U.S NAVY WORK PACKAGE." Everyspec.com, 2026, everyspec.com/MIL-HDBK/MIL-HDBK-3000-8999/MIL-HDBK-3001_16012/. Accessed 13 May 2026.

[51] DEPARTMENT OF DEFENSE. DEPARTMENT of DEFENSE HANDBOOK AIRWORTHINESS CERTIFICATION CRITERIA. 12 Dec. 2014, quicksearch.dla.mil/Transient/B2F41C30F827461EA1040B039CD5429F.pdf. Accessed Spring 2026.

[52] NAVAIR AIRWORTHINESS and CYBERSAFE PROCESS MANUAL. 2016..

[53] General Electric. "F110-GE-132 Fighter Engine Datasheet." GE Aerospace, 2024.

[54] General Electric. "F414-GE-400 Turbofan Engine Datasheet." GE Aerospace, 2022.

[55] General Electric. "GE Aerospace's XA100 Campaign Lays Foundation for Next-Gen Engines." GE Aerospace News, 2023.

[56] Pratt & Whitney. "F119-PW-100 Engine Specifications." RTX Corporation, 2024.

[57] Pratt & Whitney. "F135 Engine Product Information." RTX Corporation, 2024.

[58] MTU Aero Engines. "F414 – Military Aircraft Engines / Fighter Aircraft." MTU Product Information, 2024.

[59] FAA. "Advisory Circular 20-128A: Design Considerations for Minimizing Hazards Caused by Uncontained Turbine Engine and Auxiliary Power Unit Rotor Failure." Federal Aviation Administration, 1997.

[60] American Machinist. "Combat Aircraft Adaptive Engine Technology Advances." November 2023.

[61] Air & Space Forces Magazine. "GE Urges Pentagon to Keep Up with Adaptive Engine Tech." July 2025.

[62] Chen, H., Wang, Y., & Zhang, H. "Multi-Objective Optimization Design of Adaptive Cycle Engine with Serpentine 2-D Exhaust System Based on Infrared Stealth." Aerospace, vol. 10, no. 10, 2023, p. 858.

[63] GE Press Release — F110-GE-132 initial flight tests (2003)

[64] GE Press Release — F110-GE-132 flight test schedule (2002)

[65] Wadia & James — *F110-GE-132: Enhanced Power Through Low-Risk Derivative Technology*, AIAA (2001) — the primary technical paper on the engine's design features

[66] Wikipedia — *General Electric F110* (for general performance/heritage claims)

[67] Wikipedia — *Intake Ramp* (variable geometry intake design rationale)

[68] Aviation Week — *A Closer Look at Stealth, Part 5: Nozzles and Exhausts* (2019)

[69] Lu et al. — *Scientific Reports* (2021) on joint radar/IR stealth for exhaust systems

[70] Sun et al. — *Aerospace Science and Technology* (2021) on mixed intake/exhaust stealth design

[71] GlobalSecurity.org — Stealth aircraft IR signature reduction